

1 **Fold-thrust structures – where have all the buckles gone?**

2

3 Robert W.H. Butler, Clare E. Bond, Mark A. Cooper and Hannah Watkins

4

5 Fold-Thrust Research Group, School of Geosciences, University of Aberdeen,
6 Aberdeen AB24 3UE, United Kingdom.

7

8 **ABSTRACT:** The margins to evolving orogenic belts experience near layer-
9 parallel contraction that can evolve into fold and thrust belts. Developing cross-
10 section scale understanding of these systems necessitates structural
11 interpretation. However, over the past several decades a false distinction has
12 arisen between some forms of so-called fault-related folding and buckle folding.
13 We investigate the origins of this confusion and seek to develop unified
14 approaches for interpreting fold and thrust belts that incorporate deformation
15 arising both from the amplification of buckling instabilities and from localized
16 shear failures (thrust faults). Discussions are illustrated using short case studies
17 from the Bolivian Subandean chain (Incahuasi anticline), the Canadian Cordillera
18 (Livingstone anticlinorium) and Subalpine chains of France and Switzerland.
19 Only fault-bend folding is purely fault-related and other forms, such as fault-
20 propagation and detachment folds all involve components of buckling. Better
21 integration of understanding of buckling processes, the geometries and
22 structural evolutions that they generate, may help to understand how
23 deformation is distributed within fold and thrust belts. It may also reduce the
24 current biases engendered by adopting a narrow range of idealized geometries
25 when constructing cross-sections and evaluating structural evolution in these
26 systems.

27

28 **Introduction**

29

30 A key goal for many studies of continental tectonics is to relate folds, faults and
31 distributed strain to create reliable geometric interpretations of three
32 dimensional structure. For many decades much of this work has been allied to
33 the exploration of earth resources, especially oil and gas. Since the early 1980s,

34 descriptions of fold-thrust complexes (e.g. Suppe 1983; Jamison 1987), with
35 application to subsurface interpretation (e.g. Shaw et al. 2005), have led to
36 mechanical approaches (e.g. Smart et al. 2012; Hughes & Shaw 2015) that rely on
37 a very narrow range of deformation styles. Elsewhere we argue that this
38 emphasis has created significant bias in the ways larger-scale structural
39 interpretations are built and their uncertainties assessed (Butler et al. 2018).
40 Here we discuss how the basic concepts of buckle folding, the principles of which
41 are laid out by Ramsay (1967), may help to reduce an over-reliance on a biased
42 set of fold-thrust models. Buckling is the process by which layers fold when
43 subjected to contraction along their lengths. Research on this folding mechanism
44 has continued in parallel with that on fold-thrust belts. Our aim here is to draw
45 these lines of research together, pooling knowledge and, consequently reunite
46 interpreters of fold-thrust systems with key components in the structural toolkit
47 that is *Folding and Fracturing of Rocks* (Ramsay 1967).

48 First, we briefly outline an evolution of ideas on fold-thrust
49 interpretations – as this history underpins the majority of existing approaches to
50 folding and faulting in compressional regimes. We then examine the approaches
51 through which current understanding of buckle folds has developed in parallel to
52 these fold-thrust models. We apply these concepts to challenge the notion that
53 detachment folds and buckle folds are somehow distinct. We then examine some
54 case studies to show how buckling concepts may better inform structural
55 understanding. To unify these different approaches to better understand folding
56 and its relationship to faulting, we examine structures in terms of their evolution
57 of deformation localization. This informs a reassessment both of detachment
58 folding and fault propagation folding that sit within the family of current fold-
59 thrust models. Rather than interpret deformation in terms of idealized
60 geometries, and considering folding to be a consequence of faulting, we argue
61 that it is better to view structures as lying in a continuum of possible geometries
62 and localization behaviors (Butler 1992).

63 Much existing work examines structural evolution through cross-sections,
64 seeking explanations for fold-thrust interactions in these single illustrative
65 planes. We challenge this notion, developing concepts of lateral fold growth
66 inherent in buckling models, to argue that even if illustrated by cross-sections,

67 structural understanding is better served through considering how deformation
68 evolves in three dimensions.

69

70 **Fold-thrust structures – an introduction (the tyranny of concentric folding)**

71

72 The sedimentary rocks on the flanks of mountain belts, ancient and modern,
73 commonly show the effects of horizontal contraction, manifest as thrust faults
74 and folds. These structures have been studied for centuries – and current
75 perspectives on the developments of interpretations and concepts are provided
76 by many authors (e.g. Frizon de Lamotte and Buil 2002; Groshong et al. 2012;
77 Brandes and Tanner 2014; Butler et al. 2018). These generally recognize the
78 importance of work, especially in the foothills of the Canadian Cordillera,
79 reported by Dahlstrom (1969, 1970; but see also Fox 1959; and Bally et al.
80 1966). This was largely driven by the exploitation of oil and gas hosted in
81 complex fold-thrust structures.

82

83 Origins

84 Subsurface interpretation in frontier fold-thrust belts, be that in the
85 1960s in the Canadian cordillera of Alberta, or in the 2000s-present in the
86 Papuan fold belt (e.g. Parish 2015), is an exercise in uncertainty management. It
87 is generally driven by outcrop geology and existing wells, which provide directly
88 measured dip and horizon data, but of great complexity. This is allied with
89 regional 2D seismic profiles that, for the Canadian cordillera in the 1960s, were
90 of poor quality and thus only resolved simple structural components. In effect
91 the seismic data crudely imaged the top of the underlying basement to be gently
92 dipping, apparently planar and therefore the complex structures in the
93 sedimentary cover were detached from it. The deformation was “thin-skinned”.
94 The challenge, as met by Dahlstrom (1969, 1970), was to elaborate a workflow
95 for constructing cross-sections through the volume of thin-skinned deformation
96 that forecast subsurface structure before any further drilling. The first step lay in
97 simplification. Dahlstrom defined a narrow range of components that should be
98 used in section construction, his so-called “foothills family” of structures. These
99 are: concentric folding; décollement; thrusts (usually low angle and often

100 folded); tear faults; and late normal faults. The second part lies in testing cross-
101 section-scale interpretations for internal consistency. This was achieved by
102 structural restoration and thus the notion of balanced cross-sections was
103 formally defined (Dahlstrom 1969). In such sections, the sinuous bed-length for
104 each stratigraphic horizon measured in the interpreted structure have an equal
105 length in the pre-deformation state. Thus, restorable cross-sections are
106 demonstrations of strain compatibility – all horizons display the same
107 longitudinal strain in the section plane. When first developed by Dahlstrom
108 (1969), this method required no distortional strain within the beds (“bed-length
109 balancing”) and the strata must have been parallel-bedded before deformation
110 (so-called “layer-cake stratigraphy”). These restrictions require structures to
111 approximate to concentric folds. Subsequent development of section balancing
112 concepts have lifted these restrictions. For example, Woodward et al. (1986) and
113 Geiser (1988) discuss the incorporation of explicit strain measurements into
114 cross-section restoration and Butler (1992) developed the method of formation
115 area balancing, trading off strain-related thickness changes against pre-existing
116 stratigraphic thickness variations. Thus, interpretations could be tested using
117 structural restoration even where pre-existing stratigraphy was laterally
118 variable and distortional strain is heterogenous through multilayers.

119

120 Upscaling and downscaling

121 The success of adopting the foothills family of structures, and the rigor of
122 creating balanced cross-sections, in forecasting subsurface structure in Alberta
123 was recognized and promoted by Elliott (Elliott and Johnson 1980; Boyer and
124 Elliott 1982). In essence these approaches are about up-scaling local geology and
125 so in turn led to widespread reinvestigation of regional structure of thrust
126 systems and their relationship to orogenic belts around the world. Some of these
127 studies (e.g. Butler 1986) explicitly simplify outcrop structure by adopting the
128 foothills family to minimize the implicit values of orogenic contraction
129 experienced by thrust belts, for example, to compare with volumes of continental
130 crust beneath mountain belts. As such they make no claims of precision for the
131 structure of the thrust belts themselves.

132 Decisions on how to simplify structures on cross-sections vary depending
133 on the scientific objective. Arbitrary choices such as solutions with minimum
134 horizontal shortening may be appropriate for upscaling to deduce crustal-scale
135 tectonic processes (e.g. Butler 2013), but not if the aim is to understand the
136 relationships between individual folds and thrusts. Downscaling to forecast the
137 location of specific stratigraphic units in the subsurface, or to relate strain and
138 fracture patterns to fold development require different approaches.

139 Consequently, Dahlstrom's (1969; 1970) "foothills family" of structures was
140 developed into quantitative geometric approaches for describing relationships
141 between folds and thrusts (e.g. Suppe 1983; Jamison 1987; Mitra 1990). In this
142 way, folding is considered kinematically and thus to be a consequence of the
143 geometry, displacement and propagation of thrust faults. On this basis, Jamison
144 (1987) formalized the types of fault-related folds that can develop (Fig. 1).

145 If bed thickness is conserved during deformation, a requirement for
146 concentric folding, only a very narrow range of viable geometries also yield
147 balanced cross-sections (e.g. Suppe 1983). This restriction leads directly to
148 explicit geometric "rules" and these underpin algorithms in structural modeling
149 software (Groshong et al., 2012). In his trishear model, Erslev (1991) relaxed the
150 requirement for bed-thickness conservation - but only in the forelimb of fold-
151 thrust structures. Shaw et al. (2005) review all these models, with application to
152 seismic interpretation while Groshong et al. (2012) and Brandes and Tanner
153 (2014) review their history.

154 Just as Dahlstrom's (1969, 1970) approaches were driven by a need to
155 reduce interpretation uncertainty when forecasting the subsurface structure in
156 the pursuit of oil and gas, recent developments have also had economic drivers.
157 Many applications of fold-thrust models aim to forecast small-scale faults and
158 fractures down-scaling from larger fold-thrust structures. Consequently there
159 have been various mechanical developments from the kinematic models
160 described above (e.g. Kampfer and Leroy 2012; Smart et al. 2012; Hughes et al.
161 2014; Hughes and Shaw 2015). Note however that these mechanical models
162 generally assume a specific kinematic evolution and are applied to a single fold-
163 thrust structure, or a layer within it. The implications of adopting these
164 approaches are discussed later.

165

166 **Buckle folding – an introductory review**

167

168 Similar to fold-thrust structures, buckle folding has a history of research
169 stretching back well over half a century. However, buckling research has been
170 less concerned with forecasting poorly known subsurface structure. There are
171 several excellent discussions on buckle folding, building on the pioneering
172 studies of Ramberg (1966) and Biot (1961). Ramsay (1967) provided an early
173 overview of these works and this spawned extensive research, especially using
174 analogue materials with measurable viscosities (chiefly plasticine and gelatin).
175 Many of these results are reviewed by Price and Cosgrove (1990) who provide a
176 comprehensive account of buckling processes. Subsequently, with enhanced
177 computing capability, numerical methods have been increasingly adopted to
178 understand these processes (e.g. Abbassi and Mancktelow 1992; Mancktelow
179 and Abbassi 1992; Casey and Butler 2004; Schmalholz 2008; Reber et al. 2010).
180 Very little of this content is considered in thrust belt literature and so here we
181 provide a (re) introduction, much of which may be familiar to those currently
182 engaged in buckle research. A compilation of some buckling concepts is outlined
183 in Fig. 2.

184 For a given imposed layer-parallel contraction, the geometry of folds in a
185 single competent layer embedded in a lower viscosity matrix will depend on the
186 thickness of the layer and its viscosity in contrast to the matrix (Fig. 2a). Higher
187 viscosity contrasts favor concentric folding. Longer wavelengths are developed
188 in thicker layers. Ramberg (1966) and Biot (1961) independently established
189 that there is a cube-root relationship between layer thickness and wavelength so,
190 as Price and Cosgrove (1990), note, in multilayers of constant viscosity contrasts
191 (e.g. bedded turbidite sandstones and shales, or thick limestones with
192 interbedded shale formations), it is the thicker beds that will dictate the
193 wavelength of the resultant fold belt. They term such beds “*control units*”.

194 Single-layer buckles are encased in a deformed matrix. Based on reports
195 of analogue experiments, Ramsay (1967) illustrates how this deformation varies
196 away from a competent buckled layer through a zone of contact strain (Fig. 2b).
197 These patterns have been reproduced numerically by Reber et al. (2010; Fig 2c).

198 As the buckled layer is created by layer-parallel shortening, the long-axes of
199 strain ellipses in the zone of homogeneous strain away from the buckled layer
200 (represented by the long-dimension of the originally square elements in the
201 rectilinear grids of Figs 2 b,c) is orthogonal to the original orientation of the
202 layer. In nature this attribute will be tracked by axial-planar cleavage associated
203 with the folds.

204 Based on approaches of Latham (1985; reviewed by Price and Cosgrove
205 1990), Casey and Butler (2004) argue for a complex evolving relationship
206 between strength and imposed shortening (Fig. 2d). Planar competent layers
207 have a bending resistance that must be overcome if folds are to amplify
208 significantly. This is particularly important for anisotropic materials – such as
209 well-bedded units. Once bending resistance is overcome, folding is efficiently
210 achieved through near-rigid limb rotation. Stress increases initially until the
211 bending resistance of a layer is overcome, at which point there can be a dramatic
212 stress drop throughout this deforming layer. Deformation can progress readily
213 by limb rotation until limited by interlimb angle. Folds will then tend to lock up.

214

215 Faulting and folding

216 Rheological multilayers can deform by buckling and thrusting. Although
217 these are distinct forms of mechanical instability, extensive analogue modelling
218 (reported by Price and Cosgrove 1990) demonstrates that these can co-exist
219 during the same deformation (Fig. 2e). Continued deformation may result in
220 faults propagating into previously unfaulted, folded layers, or becoming shut-
221 down and folded if adjacent buckles amplify appropriately.

222 Using well-exposed coastal outcrops along the flanks of Oslo Fiord,
223 Morley (1994) describes arrays of thrusts that apparently relate to over-
224 tightening of fold hinges, rather than having formed as linked fault networks.
225 Morley's interpretations are a rare published example that folds can contain
226 minor faults, despite their description by Ramsay (1967, p. 421). Price and
227 Cosgrove (1990) class these as accommodation structures (Fig. 3a, b). They note
228 that such structures tend to concentrate in the hinges of folds and are
229 preferentially developed in competent layers adjacent to thicker beds (control
230 units) that are dictating the overall fold shape (Fig. 3c). The types of faults are

231 characteristically rootless and pass onto segments of bedding planes. Examples
232 include “out-of-syncline” thrusts (Dahlstrom 1970).

233 There have been a few attempts to identify accommodation faults in
234 thrust belts. Mitra (2003) reports many examples, including within the Ventura
235 Avenue Anticline of Southern California (Fig. 3d). Well data reveal multiple
236 thrusts that accommodate thickening of the Pico Formation (Pliocene), yet these
237 thrusts appear not to cut deeper horizons or continue to outcrop. Similar
238 behavior is interpreted by Boyer (1986) in his consideration of the Anschutz
239 Ranch East Field in the Wyoming Overthrust Belt (Fig. 3e). Here too, well
240 penetrations identify complex faulting along the hinge of a tight fold within the
241 Preuss/Stump Formation (Jurassic). The fold appears to be controlled by a
242 competent layer at depth defined by the Nugget Sandstone and Twin Creek
243 Limestone. The accommodation fault passes into incompetent evaporites.

244

245 Fold trains

246 In contrast to the fold-thrust structures presented earlier (Fig. 1), buckle
247 folds are generally not considered in isolation, but rather as arrays. For example,
248 analogue experiments by Dubey and Cobbold (1977) demonstrated that folds
249 form in trains and that they propagate laterally as they amplify (Fig. 4a, b). The
250 initial fold systems initiated in clusters on inherited flaws in the plasticine
251 multilayer. However, these clusters grew out laterally. Folds from different
252 clusters can collide. Where folds are in phase they can combine to create long,
253 fully-connected hinge lines. Fold mergers like this, although long recognized, are
254 similar to behaviours more recently deduced for segment-linkage in the
255 formation of large normal faults (e.g. Cartwright et al. 1995). However, other
256 folds may remain segmented generating abrupt plunge terminations (see also
257 Casey and Butler 2004; Fernandez and Kaus 2014). Progressive deformation
258 establishes a dominant wavelength of the fold train, overprinting the initial
259 distribution of perturbations that may have seeded the initial folds.

260

261 Multilayer fold trains

262 Dixon and Lui (1992) performed folding experiments in analogue
263 materials that demonstrate the lateral growth of buckle systems. The model

264 illustrated here (Fig. 5a, b) shows a series of three thick competent layers (X, Y,
265 Z) separated by low-viscosity material within which is encased a highly
266 competent marker (contorted blue line in Fig 5a, b). Comparison of the two
267 deformation states (Fig. 5a evolves into Fig. 5b) shows how the folds grow.
268 Although the multilayer contains low viscosity levels, the folds in the competent
269 units are broadly in harmony. The experiment shows, that although folds may
270 grow across a model (Fig. 5a, b), once formed, they can amplify together. The
271 overall fold train geometry is controlled by the thicker units, confirming the
272 reports by Price and Cosgrove (1990). The models also illustrate how the
273 structure of fold hinges in these control units (X, Y, Z) can influence deformation.
274 Consider fold III in Fig. 5b. The upper layer (X) has ruptured by crestal faulting
275 allowing the fold limbs to rotate, greatly decreasing the interlimb angle. This in
276 turn influences the structure of the underlying thin layer. In nature, these
277 behaviours would likely be facilitated by erosion of the antiform crest. It is not
278 just the upper layer (X) that develops tight folds. The middle control unit (layer
279 Y) has tight interlimb angles (e.g. folds IV and VI in Fig. 5b). These layers are
280 locally faulted in their forelimbs.

281 Multilayer folding has also been investigated in 3D finite element models.
282 The examples shown here (von Tscherner et al. 2016; Fig. 5c, d) illustrate the
283 stratigraphic control on disharmonic deformation. Here buckling is developed in
284 competent units against a step that mimics a basement fault. If the incompetent
285 matrix (green in Fig. 5c, d) is thick above the basement then the two competent
286 layers can fold harmonically. A thinner low-viscosity layer immediately above
287 the basement promotes disharmonic deformation.

288

289 **Detachment folding and buckle folding: a false distinction?**

290

291 Groshong (2015) makes an explicit distinction between detachment folds and
292 buckles, although both systems can develop above fixed décollement levels. For
293 his definition of detachment folding, the antiforms rise away from the
294 décollement, creating an “excess area” beneath a specific horizon that is equal to
295 the amount of horizontal shortening multiplied by the height of the horizon
296 above the detachment away from the fold (Fig. 6a). In contrast, he conceptualizes

297 buckling with uplift of the anticline crest but with net subsidence beneath
298 synclines (Fig. 6b). Likewise, Mitra (2003 see also Ghanadian et al., 2017)
299 illustrates buckling of above décollement surfaces where ductile material is
300 evacuated beneath synclines and flows into anticline hinges.

301 Note that the basic conceptualization of buckle folding (Figs 2b, c),
302 developed both from analogue experiments and from numerical modeling, does
303 not show evacuation beneath synclines. Consider the state of finite strain around
304 single layer buckle folds. Some classical buckling models (e.g. Fig. 2b) depict
305 outer-arc stretching tangential to fold hinges (e.g. Ramsay 1967; Price and
306 Cosgrove 1990). However, these strain states are restricted to within, or are
307 immediately adjacent to, competent layers. More generally, single layer buckles
308 are shown to pass out into homogeneous strain that accommodates shortening
309 (Figs 2b, c). As noted earlier – this predicts axial planar cleavage – in antiforms
310 and synforms alike. If Groshong's (2015) assertions are correct, in regions of
311 horizontal sub-contraction, cleavage would be axial planar in the antiforms (near
312 upright) but sub-perpendicular to synform axial surfaces (near horizontal).
313 These relationships are certainly not generally observed in regions of distributed
314 folding, such as slate belts (e.g. Coward and Siddans 1979; Woodward et al.
315 1986).

316 Perhaps the confusion of buckling has arisen because of the way in which
317 results of analogue experiments have been reported. This is illustrated in Fig 6c,
318 using an experiment of progressive deformation described by Cobbold (1975, fig.
319 5) on buckling in heterogeneous paraffin wax. His images are redrafted here in
320 colour with added labelling for reference. The original model was set up with a
321 single competent layer (X on Fig. 6c), embedded within a matrix of lower
322 viscosity upon which were printed reference lines, parallel to the competent
323 layer and the lower edge of the deformation apparatus. One of these reference
324 lines is labelled here (Y on Fig. 6c). The aim of Cobbold's study was to chart the
325 amplification of folds and so his illustrations focus on the buckled competent
326 layer itself (X on Fig. 6c), centered through the middle of the growing fold.
327 Consider the low strain state with the left-hand high strain image (Fig. 6c) - the
328 frame of reference of the initial location of the competent layer relative to the
329 deformation apparatus is lost. Cobbold's images are cropped, as evidenced by the

330 trimming of the printed pre-deformation reference lines between successive
331 deformation states. If the images are rehung relative to the pre-deformation
332 reference lines (e.g. Y on Fig. 6c), the control layer X is shown to have moved
333 upwards (right hand high strain state in Fig. 6c). There is no subsidence of the
334 synforms and the surrounding deformation is broadly as described by Ramsay
335 (1967, Fig. 2a) and others since.

336 The key for analysing fold development is to relate the deformation of a
337 layer to its “Regional”. The term “*Regional*”, as applied to a deformed horizon and
338 formalized by Williams et al. (1989), is short-hand for “regional orientation and
339 elevation” of that horizon at a scale significantly greater than of a particular
340 deformation structure. It is easiest to apply in sedimentary basins, where the
341 “regional” describes the very long-wavelength of a particular horizon. The
342 behavior of the horizon relative to its “regional” is diagnostic of tectonic regimes.
343 Extensional faulting drops rocks below their regional. Contractual faulting
344 brings rocks above their “regional”. These are net behaviours and are especially
345 useful for analyzing reactivation of faults (see Williams et al. 1989). As implied
346 by the strain state shown by Ramsay (1967, p. 417), the folded competent layer
347 is raised above its “regional” throughout. It is differential but still upward
348 movement of the buckled layer that creates antiforms and synforms. Nowhere in
349 the model is there subsidence.

350 The “regional” concept can be applied to the analogue model experiments
351 in Fig. 6c. Here it is the mis-identification of the “regional” for the base of the
352 competent layer (X) in the left-hand illustration that leads to the false deduction
353 of synform subsidence. When the higher strain state is rehung using the deeper
354 marker horizon (Y, the right hand illustration), the “regional” for the base of the
355 control layer moves down. This is a minimum illustration for the location of the
356 “regional”, because if the levels in the model beneath the marker horizon are
357 involved (as they were, when considering the low-strain state), the original
358 location of the control layer (X) would move further down still. This example is
359 consistent with the illustrations of Ramsay (1967; Fig. 2a).

360 In areas of no imposed longitudinal strain, rocks can still move relative to
361 their “regionals” as a consequence of redistribution of material at depth, for
362 example due to salt flow. In this case, subsidence beneath salt-withdrawal basins

363 (a pre-kinematic stratum goes below its “regional”) is compensated for by uplift
364 of a salt pillow (the same pre-kinematic stratum goes above its “regional”). It
365 appears to be characteristic of systems that have a thick layer of exceptionally
366 low-viscosity material at depth. Subsidence of synclines is driven by deposition
367 of syn-kinematic strata – so-called “down-building”.

368 Simpson (2009) provides results from numerical modelling that explores
369 the geometry of fold and thrust structures that form above low-viscosity layers
370 in decollement zones (Fig. 6 d, e). These models use exceptionally low viscosities,
371 perhaps appropriate to salt or over-pressured mud. Deformation of the
372 competent beam above this material generates arrays of buckle folds together
373 with localized shears, equivalent to thrusts. Where the low-viscosity zone is thin,
374 the synclines in overlying competent units remain above their “regional” (Fig.
375 6e). In contrast, where the low-viscosity zone is thick, the synclines subside
376 below their “regional” (Fig. 6d) While these behaviours may be appropriate to
377 some submarine thrust systems at the toes of gravitationally spreading
378 sedimentary prisms, it is not obvious that these models are applicable to
379 foreland fold and thrust belts. Exceptions may include those fold belts that
380 include thick evaporite sequences at depth, such as the Provencal sector of the
381 French Alps (Graham et al. 2012) and the Fars sector of the Zagros (e.g.
382 Mouthereau et al. 2007). Note that syncline subsidence during folding generates
383 growth stratal patterns that are distinct from normal buckling (contrast Figs 6d
384 and e), as identified by Oveisi et al. (2007) in their modelling of deformed marine
385 terraces along the frontal folds of the central Zagros.

386 In summary, the vertical motion of synclines relative to their “regional” is
387 not controlled by the folding mechanism, as proposed by Groshong (2015), but
388 the ductility of the deeper parts of a deforming stratigraphic section. The
389 distinction between detachment folding and buckling on these grounds is false.

390

391 **The Incahuasi anticline as a buckle fold**

392

393 In the oil and gas industry, the effectiveness of structural interpretations on the
394 scale of cross-sections is repeatedly tested by drilling. However, being
395 commercially sensitive, interpretation failures are rarely reported. An honorable

396 exception is Total's development history of the Inchuasi structure in the
397 SubAndean fold belt of Bolivia (Heidmann et al. 2017; Fig. 7).

398 The target for exploration drilling has been the porous sandstones of the
399 Huamampampa Formation (Devonian) that host major gas reserves. These
400 underlie the Los Monos Formation (Devonian), a shale-prone unit that forms a
401 top-seal. It also acts as a ductile unit across which deformation changes (e.g.
402 Rocha and Cristallini 2015, and references therein). The overlying Carboniferous
403 to late Cretaceous units appear to deform as a single competent beam. At outcrop
404 these strata form a fold-belt with remarkable lateral continuity of anticline
405 hinges (>200km) separated by synclines that host Tertiary syn-kinematic
406 foredeep sediments (Fig. 7a). The Huamampampa Formation lies at the top of a
407 Silurian-Devonian package that is generally assumed to deform as a single unit,
408 detached from the underlying basement along the Upper Silurian Kirusillas
409 shales. Prior to Total's drilling campaign there had been various attempts to
410 forecast subsurface structure of the fold-belt using analogues models (e.g.
411 Leturmy et al. 2000; Driehaus et al. 2014; Darnault et al. 2016), generally
412 preconditioned to create a two-tier thrust system decoupled along the Los
413 Monos Formation.

414 Two-tier deformation formed the initial subsurface model for Total's
415 drilling (Fig. 7b). The target was the crest of a proposed hangingwall anticline in
416 the underlying thrust system. However, this first well penetrated a faulted
417 anticline and was terminated in Cretaceous strata on the western limb of the
418 fold. In the light of this result, the structural interpretation was modified (Fig. 7c)
419 and a side-track well proposed to target the deeper structure. As this side-track
420 was drilled, rather than encounter the Huamampampa Formation in the crest of
421 a simple anticline, these sandstones were found to be faulted and locally over-
422 turned. Consequently, the structural interpretation was modified again (Fig. 7d).

423 The history of iterative subsurface interpretation and drilling on the
424 Incahuasi structure is interesting. As knowledge was gained, the role of the Los
425 Monos Formation as a significant zone of structural decoupling reduces. At the
426 start of the drilling campaign the Carboniferous-Cretaceous upper stratigraphic
427 beam is interpreted to be entirely decoupled from the Silurian-Devonian beam
428 below and each has its own structural style. By the end of the campaign, the

429 Huamampampa Formation is interpreted as folded, broadly in harmony with the
430 upper beam. A further detachment horizon, located within the Icla Formation,
431 has been incorporated by Heidmann et al. (2017) so that the older Devonian and
432 Silurian strata can shorten by simple fault-bend folds. But does the structural
433 style need to vary with depth, from buckle folding at shallow levels and fault-
434 bend folding at depth?

435 The Incahuasi anticline is re-assessed here using some buckling concepts
436 (Fig. 8). This new interpretation has been balanced, so that all formations show
437 the same horizontal contraction. The upper units of Carboniferous to Cretaceous
438 age are illustrated as acting as the control unit (in the sense of Price and
439 Cosgrove 1990). Rather than interpret the Los Monos Formation as a mechanical
440 detachment (c.f. Heidmann et al. 2017), we suggest that it represents a
441 transitional strain zone across which there is broad structural continuity. The
442 underlying Devonian and Silurian strata are also shown to fold harmonically
443 with the upper units, with localized accommodation faulting in the anticline
444 hinge. It is these faults that were encountered as the sidetrack well entered the
445 Huamampampa Formation. The fold may also continue below this unit too, so
446 that the whole stratigraphic pile deforms as a single entity.

447 Our model differs from that of Heidmann et al. (2017). We suggest that
448 the older Silurian rocks are not involved in the Incahuasi structure and there is a
449 décollement surface within the lower Devonian rocks (Icla Formation) beneath
450 the Huamampampa reservoir unit. This version conserves the cross-sectional
451 areas of different formations between deformed and undeformed states
452 (achieves formational area balance). It is possible that the deeper Silurian strata
453 are involved – especially if deformation in these deep levels was largely
454 homogeneous layer-parallel shortening. Testing this interpretation requires
455 knowledge of the “regional” for the various stratigraphic units in the Incahuasi
456 structure. The long section in Fig. 7a provides some insight. The base of the
457 synclines in the upper beam of Cretaceous and younger strata, the lower
458 enveloping surface of the folds, inclines gently west. However, if there has been
459 deformation in the underlying Silurian and Devonian strata, this enveloping
460 surface does not constitute a “regional”. Information is needed for deeper

461 basement trends and the position of horizons in the foreland – information that
462 lies beyond the scope of even the long section reproduced in Fig. 7a.

463 If the Subandean fold and thrust belt of Bolivia, incorporating the
464 Incahuasi anticline, are best considered as a train of buckle folds, we can apply
465 the concepts of fold amplification of Casey and Butler (2004, Fig. 2e). Erosion of
466 the anticline fold crests could have a critical influence on the amplification and
467 tightening of folds, allowing deformation to progress beyond the expected lock-
468 up interlimb angle (as shown in the analogue experiments of Dixon and Liu
469 1992; Fig. 5b). In contrast, sedimentation in the synclines could inhibit the
470 growth of further anticlines between the existing folds, enhancing those
471 structures that had already formed.

472

473 **Cyclic folding and faulting – the Livingstone anticlinorium**

474

475 Kink-band folding, accommodated by flexural slip, is the generally-
476 accepted mechanism for the formation of structures in the foothills of the
477 Canadian cordillera (Dahlstrom 1970). Tight kink anticlines in the hangingwalls
478 to thrusts are conventionally interpreted as fault-propagation folds that have
479 evolved and been carried by the thrust. Cooley et al.'s (2011) interpretation of
480 the Livingstone anticlinorium of the foothills of the Canadian cordillera (Fig. 9)
481 challenges this notion. The anticlinorium is a composite array of folds associated
482 with the Livingstone Thrust. The strata are dominated by well-bedded
483 Mississippian carbonates typical of this part of the Alberta foothills. Cooley et al.
484 (2011) mapped the folds and, supported by detailed fracture studies and
485 diagenetic histories of vein fills, deduce the deformation history. The Central
486 Peak anticline initiated at depth, in parallel to the growth of the Livingstone
487 Thrust. In this sense, it is a thrust-propagation fold. However, the anticline
488 tightened after the thrust had accumulated its displacement. The structure has a
489 two-stage history.

490 The history of the Livingstone anticlinorium contrasts with the idealized
491 evolution of fault-propagation folds. The results of Cooley et al. (2011) indicate
492 that deformation need not evolve as a simple passage from distributed folding to
493 localized thrusting but rather it can cycle between these different localization

494 behaviors. Similar patterns have been deduced for fold-thrust complexes in the
495 French Subalpine chains (e.g. Butler and Bowler 1995). Interacting folds and
496 thrusts are also modelled numerically by Jaquet et al. (2014). Cycling between
497 localized thrusting and distributed folding has important implications for some
498 hydrocarbon systems as it could change the timing of the development of
499 fractures in prospective subsurface reservoirs relative to the timing of
500 hydrocarbon charge. It could also compromise the integrity of seals.

501

502 **3D folding – the nucleation problem.**

503

504 Early work on analogue materials demonstrated that buckle fold trains can
505 initiate on pre-existing heterogeneities (Dubey and Cobbold 1977). This notion
506 can be explored using the folds of the Subalpine chains and Helvetics of the NW
507 Alps. Structures are developed in the multilayer of thick Mesozoic platform
508 carbonates interbedded with shale-prone formations (Fig. 10). The youngest
509 carbonate platform, termed the Urgonian limestone (Hauterivian-Barremian)
510 forms regional folds with hinge lines that can be traced over tens of km (e.g.
511 Ramsay 1989). Folding in the Urgonian is apparently out-of-phase with
512 structures in the underlying units, for example the competent Tithonian
513 limestones (Fig. 10). In the Subalpine fold belt, two formations are separated by
514 thick lower Cretaceous shales. Jurassic strata below the Tithonian limestone are
515 also shale prone and thick. These stratigraphic successions are inherited from a
516 Mesozoic basin section. In contrast, to the west the fold-thrust belt involves an
517 interbedded succession of thick platform carbonates and thin shales.
518 Consequently in this western area the stratigraphy deforms harmonically and
519 the role of major buckling appears to be less important (Fig. 10; see Butler et al.
520 2018, for further discussion).

521 Within the Subalpine system, anticlines in the Urgonian limestone at
522 several locations coincide with pre-existing normal faults. Two examples are
523 shown here, from either end of the system. In the Vercors, a single east-dipping
524 normal fault can be reconstructed from the folded Urgonian (Fig. 11a; Butler
525 1987). At the Col de Sanetsch in the Helvetic Alps of Switzerland, the Urgonian
526 limestone is folded into a NW-facing fold pair. It contains arrays of SE-dipping

527 normal faults that are overlapped by Tertiary strata deposited before folding (Fig.
528 11b). In both of these cases the normal faults have throws that are less than the
529 thickness of the Urgonian limestone. Nevertheless, it is tempting to suggest that
530 these pre-existing faults were sufficient to nucleate folding. Presumably the folds
531 propagated laterally from these inherited flaws in the Urgonian beam to create
532 the connected fold trains of the Subalps, as modelled in von Tscharner et al
533 (2016).

534 Figure 12 is a hypothetical illustration of fold nucleation and growth.
535 Isolated arrays of small normal faults, equivalent to those illustrated in Fig. 11,
536 were developed before folding. They act as perturbations, in the sense of Dubey
537 and Cobbold (1977) to nucleate early fold growth (Fig. 12b). As layer-parallel
538 shortening continues, some of the folds amplify and propagate their hinges
539 laterally – eventually to connect into a continuous fold train (Fig. 12c). This
540 raises an important issue when considering an individual cross-section through
541 a fold-belt. Explanations of the spatial distribution of specific folds or structural
542 styles may lie outside the cross-section or structure of interest. A holistic
543 consideration of the fold-thrust belt may be more informative.

544

545 Implications for modeling strategies

546 There have been various attempts to mimic the fold patterns of the Subalpine
547 and Helvetic Alps (e.g. von Tscharner et al. 2016). These represent a
548 considerable advance on approaches that impose a kinematic model to a
549 multilayer to reproduce deformation within the Urgonian limestone (e.g. Smart
550 et al. 2012). in that they are three dimensional. They do however use flawless
551 rheological beams. Yet, if the results from analogue models of Dubey and
552 Cobbold (1977) are generally applicable, buckle fold clusters nucleate on
553 perturbations thus the initial fold pattern will develop from the amplification of
554 these pre-existing heterogeneities. It is only at rather significant bulk contraction
555 (>35%) that the fold system self-organizes with dominant wavelengths
556 controlled by layer-thicknesses. If taken into the natural world, this implies
557 almost all foothills systems are still under the influence of their heterogeneities.
558 Perhaps the deformation of sedimentary multilayers is comparable to mineral

559 physics – it is the existence of lattice defects that allows crystals to deform
560 plastically (e.g. Nicolas and Poirier 1976, p. 52).

561

562 **Comparing approaches**

563

564 The folded Mesozoic strata of the Jura mountains of Switzerland were
565 interpreted by Buxtorf (1916), largely using outcrop, well data and then-new
566 railway tunnels. His cross-section (Fig. 13) shows variations in deformation
567 localization, while retaining a common feature of decoupling of the cover rocks
568 from the underlying basement. In this regard, his cross-section is similar to those
569 considered by Dahlstrom (1970) in the Canadian foothills. Both view the
570 deformation as thin-skinned. Buxtorf's interpretation of the structure beneath
571 the Grenchenberg tunnel (Fig. 13) is amongst the most widely reproduced in
572 structural geology. This section and its subsequent reworking was much cited as
573 an example of buckle folding above a basal decoupling surface (e.g. Ramsay
574 1967). Subsequently it has become a much-cited example of detachment folding,
575 featuring in text books such as Fossen (2016). Likewise, the various other fold-
576 thrust models illustrated in Figure 1 all have long heritage. Fault-bend folds (Fig.
577 1a) were famously interpreted in the Appalachians by Rich (1934). The notion
578 that thrusts grow as strain localizes in folded strata, the feature of fault-
579 propagation folding (Fig. 1b; Williams and Chapman 1983), goes back to at least
580 to Willis (1894) and Heim (1878). However, since the early 1980s, although
581 these historical roots are often cited, the descriptions of structural geology
582 surrounding them, have become blurred. Thus, the now-prevalent terminology
583 of fault-related folding, outlined on Fig. 1, has been increasingly used to develop
584 structural interpretations, without addressing underlying issues, especially
585 concerning buckling instabilities and distributed strain.

586

587 Evolving literature and confirmation bias

588 Figure 14 charts the increase in the application of idealized fold thrust
589 geometries as depicted on Fig. 1, from the early 1980s to the present. It also
590 shows the publication of research on buckle folds, sourced from the online tool
591 Scopus - Elsevier's abstract and citation database, for the same period. Cursory

592 inspection may suggest that, if the literature reflects geological reality, the
593 dominant style of deformation is detachment folding and that there are relatively
594 few buckle folds. What are the implications of this? Are detachment folds distinct
595 from buckle folds? Are true buckle folds rather rare? Can cross-sections across
596 mountain belts like the Jura be reliably constructed using simple methods and
597 folding concepts (e.g. Poblet and McClay 1996; Mitra 2003; Shaw et al. 2005)?

598 We argue below that the distinction between detachment folding and
599 buckle folding above a décollement is false. Hence, much of the literature
600 represented in Fig. 14 simply follows the newer categorization of detachment
601 folds, as part of the fold-thrust belt model suite, rather than buckle folding. The
602 effect is to polarize structural geologists and risks detaching those engaged in
603 subsurface interpretation from a rich vein of knowledge.

604 The use of categorization of concepts and associated nomenclature can be
605 useful standard scientific practice to aid communication and to share analogues.
606 Applications include fossils (e.g. Woodward 1885), plants (e.g. Jones and
607 Luchsinger 1979) and minerals (e.g. Morimoto 1988; Leake et al. 1997).
608 Grouping in this way generally implies associations within categories and is
609 appropriate when these objects are similar. However, the approach can promote
610 studies that seek to confirm existing understanding at the expense of those that
611 seek to challenge conventional wisdom. This is termed “confirmation” bias,
612 unwitting selectivity in the acquisition and use of evidence (Nickerson 1998),
613 which is compounded by the availability of models - “availability bias”. These
614 type of bias are widely recognized in scientific investigations (e.g. Mynatt et al.
615 1977) and can restrict the range of concepts or models chosen to explain natural
616 phenomena. Alcalde et al. (2017) show the impact of a limited range of training
617 examples on interpretations of a fault in a seismic image. If the findings of this
618 paper are generically applicable, today’s structural geology students, brought up
619 on a diet of post 1990 text-books and sub-surface interpretation manuals, will
620 invariably interpret structures such as those on Buxtorf’s cross-sections through
621 the Jura (Fig. 13) as detachment folds and name them as such, rather than
622 consider them to be buckle folds. It is perhaps unsurprising therefore that
623 examples of natural structures or their interpretations illustrated on cross-
624 sections that conform to the specific styles illustrated in Fig 1 are widely

625 documented. Alternative approaches and observed structural geometries may be
626 under-reported or poorly cited in published literature. Such bias is increased by
627 reliance on modeling software that only allows for a narrow range of
628 deformation modes for cross-section construction (Groshong et al. 2012).
629 Perhaps the reliance on simple kinematic descriptions of fold-thrust complexes
630 charts the increasing use of seismic reflection data to construct cross-sections
631 through the subsurface. In this context, conventional structural interpretation
632 strategies emphasize beds, the continuity of stratal reflectors and their offsets
633 across faults (but see Iacopini and Butler 2011).

634 So consider this rationale: fault displacement and bed-length can be
635 measured and sections constructed and restored accordingly; deformation
636 distributed strain cannot be readily detected or quantified; therefore the
637 possibility of strain is ignored; so bed deformation is assumed to have occurred
638 by concentric folding alone. The resultant cross-section is restorable and thus is
639 assessed as carrying a low risk of being wrong, certainly compared with
640 unrestored interpretations. But this risk assessment would rely on arbitrarily
641 negating the significance of distributed deformation and focusing exclusively on
642 interpretations that are restorable using purely concentric folding and fault slip.
643 As such it is unreliable.

644 The above scenario is an example of the McNamara Fallacy, a form of
645 cognitive bias that engenders over-confidence in a particular deduction (e.g. Bass
646 1995). It is a widely recognized syndrome resulting from over-reliance on a
647 narrow range of data, generally the most-readily quantitative, at the expense of
648 factors that are less amenable to quantification (e.g. Martin 1997; O'Mahony
649 2017). In our scenario, the bias lies in retaining only a narrow range of possible
650 structural geometries and relegating others as being irrelevant complexities -
651 only adopting modeling solutions that follow a few numerical approximations
652 while ignoring interpretation possibilities that cannot be so simply modelled.
653 The challenge then is to increase the availability of models and approaches,
654 rather than rely on a narrow, over-defined set of possible solutions.

655

656 **Localisation – forced folds vs buckle folds**

657

658 Here we develop a broader basis for understanding relationships
659 between folds and thrusts, linking the idealized fold-thrust models (Fig. 1) to
660 buckle fold concepts (Fig. 2). Our aim is to provide a more holistic view of
661 deformation, and deformation localization in compressional settings that better
662 considers the true structural evolution of folds, faults and their interplay in
663 multi-layered stratigraphy. Notwithstanding the issues raised above, we restrict
664 discussions here to cross-sections, but recognize the importance of adopting 3D
665 approaches for understanding structural evolution (but see Butler 1992).

666 Consider layer-parallel contractional deformation acting upon a sequence
667 of parallel-bedded strata (Fig. 15). We can chart the distribution of deformation
668 within an individual layer with respect to the aggregation of shortening. For
669 ideal fault-bend folding, a fault nucleates instantly so deformation is localized
670 onto an infinitesimal small part of this layer. As shortening increases
671 displacement remains entirely localized (Fig. 15). Note that in the hangingwall to
672 the fault, the layer is deformed, simply as a consequence of displacement. Fischer
673 and Coward (1982) quantify these flexural flows. As Cosgrove and Ameen (1999;
674 following Stearns 1978) note, this is an example of *forced folding* – a
675 consequence of displacements in the surrounding rocks. They draw distinction
676 between folds formed as a consequence of compression acting parallel to
677 layering – *buckles*. In these systems a single horizon never localizes a thrust
678 ramp but simply, the strata above the detachment, décollement, or thrust flat
679 continues to accommodate deformation by folding. If the layer retains constant
680 thickness during deformation, folding in that layer must be accommodated by
681 rotation and, as noted previously (Butler 1992), if there is a fixed décollement
682 surface, there must be hinge migration. Consequently, the amount of rotated bed
683 must increase as shortening is accommodated (Fig. 15). Williams and Chapman
684 (1983) developed a general strain case so that layer thickness can change during
685 deformation.

686 We can consider the two behaviors discussed above to represent end-
687 members (Fig. 15) – either: (i) instantaneous displacement localization or (ii)
688 distributed folding continuing through the entire deformation history. However,
689 fault-propagation folding envisages deformation evolving so that a layer first
690 deforms by folding but then localizes displacement as a thrust grows into it (see

691 Mitra 2003 and many others). This chronology may be an expression of strain
692 hardening. But the universal relevance of this model is challenged by the study of
693 Cooley et al. (2011) discussed above (Fig. 9). Folding happened both before and
694 after movement on the Livingstone Thrust.

695 The concept of mechanical stratigraphy is used by some to assess strain
696 development (especially fracture patterns) assuming larger-scale structural
697 geometries and evolutions that build upon concepts of fault-related folds (e.g.
698 Smart et al. 2012; Hughes et al. 2014). Using the terminology of Cosgrove and
699 Ameen (1999) – these are effectively viewed as forced folds as distinct from
700 buckles. This view is reinforced by contributions from Groshong (2015). The
701 implication is that buckling is a rare process in fold-and-thrust belts. Yet buckle
702 folds and forced folds have different mechanics and yield different forecasts of
703 fracture and other strain patterns (discussed by Cosgrove and Ameen 1999).
704 Failure to consider buckling processes will make inappropriate fracture
705 forecasts, of structurally controlled fractures.

706

707 **Discussion: where have all the buckles gone?**

708

709 For decades, most studies of fold-thrust belts have considered folding to
710 be a consequence of thrust geometry and faulting processes. The implication is
711 that layer buckling is a rare process in fold-and-thrust belts. We have argued
712 here that this is wrong – and that there is a spectrum of folding and faulting
713 styles that can co-exist in stratigraphic multilayers. To answer our titular
714 question: the buckles are still there. In many studies over the past 25 years,
715 structures which have involved components of layer buckling have simply been
716 renamed as fault-propagation or detachment folds. But through renaming,
717 swathes of relevant knowledge on buckling systems has been largely neglected,
718 not only by communities striving to interpret and forecast the subsurface, but
719 also by those attempting to down-scale to forecast patterns of fracture and strain
720 within folds.

721 The use of restricted structural styles in cross-section construction was
722 strongly criticized by Ramsay and Huber (1987; p. 557), although wrongly
723 conflated with the concept of section balancing. Simplification is an inherent

724 process in most scientific investigation – its appropriateness depends on the
725 specific problem under investigation. So the reasons for adopting particular
726 geometric solutions depend on the purpose of a particular cross-section or
727 modeling campaign.

728 Ramsay (1967), in developing mathematical approaches to quantify the
729 geometry of deformed rocks, focused on spatially continuous strain. Up-scaling
730 emphasizes strain compatibility so that heterogeneous strains change gradually
731 through a deformed rock volume. In contrast, the development of thrust
732 concepts has emphasized discontinuous deformation and characterizes these
733 discontinuities – the thrust faults. Up-scaling and the consideration of strain
734 compatibility underpins the notion of section balancing. But by emphasizing
735 displacement and the associated forced folds, the role of distributed strain and
736 buckling have been neglected. Buckle folds and forced folds have different
737 mechanics and yield different forecasts of fracture and other strain patterns
738 (Cosgrove and Ameen 1999). There was once extensive research on strain
739 patterns in thrust sheets (e.g. Coward and Kim 1981; Morley 1986; Woodward et
740 al. 1986; Geiser 1988; Mitra 1994) that sought to quantify distributed
741 deformation alongside thrust displacements. However, there are few such
742 studies today.

743 The problem of over-confidence in structural interpretation is
744 compounded by publications, as illustrated on Fig. 14 . As a structural geology
745 community we should consciously challenge our interpretations that conform to
746 ‘classic’ rules and geometries. In this way we may limit further bias in our
747 interpretations of fold-thrust structures and cease contributing further to
748 availability bias (Bond et al., 2007; Alcalde et al. 2017).

749 Interpretations biased from adopting Dahlstrom’s “foothills family”, and
750 the derivative range of fold-thrust models (e.g. Shaw et al. 2005; Fig. 1), can be
751 managed if the purpose is to up-scale from structural interpretations. This might
752 be to evaluate tectonic processes through obtaining estimates of shortening of
753 rocks in the upper crust, if quoted as minima, or a range of likely values rather
754 than single determinations (e.g. Elliott and Johnson 1980; reviewed by Butler
755 2013). Or it could be to develop predictions of the large-scale thermal evolution
756 of thrust belts (e.g. Deville and Sassi 2005; McQuarrie and Ehlers 2017).

757 However, understanding the evolution of folds, predicting smaller-scale
758 structures within specific layers and forecasting their geometry in the
759 subsurface, are hindered by considering only a narrow range of deformation
760 modes. The history of exploration drilling for hydrocarbons in thrust systems
761 bears testimony to these inherent uncertainties (Butler et al. 2018), as typified
762 by our discussion of the Incahuasi structure (Fig. 7). Understanding the risks of
763 interpretation failure and the construction of cross-sections that improve
764 predictions of subsurface structure, may be enhanced by better integration both
765 of information on the heterogenous localization of strain within layered
766 sequences and of buckle folding concepts into fold-thrust models.

767

768 Acknowledgements

769 We dedicate the paper to the memory of Martin Casey (1948-2008), who did
770 much through good-humored argument to ensure that buckling ideas were not
771 lost to what he called “the Ramping Club” (the thrust belt community). The Fold
772 – Thrust Research Group has been funded by InterOil, OilSearch and Santos. We
773 thank Paul Griffiths and anonymous referee for comments together with
774 Hermann Lebit for scientific editing. The views expressed here of course remain
775 those of the authors.

776

777 **References**

778

779 Abbassi, M.R. and Mancktelow, N.S. 1992. Single layer buckle folding in non-
780 linear materials—I. Experimental study of fold development from an isolated
781 initial perturbation. *Journal of Structural Geology*, **14**, 85-104.

782

783 Alcalde, J., Bond, C.E., Johnson, G., Butler, R.W.H., Cooper, M.A. and Ellis, J.F. 2017.
784 The importance of model availability on seismic interpretation. *Journal of*
785 *Structural Geology*, **97**, 161-171.

786

787 Bally, A. W., Gordy, P. L., Stewart, G. A., 1966. Structure, seismic data and orogenic
788 evolution of southern Canadian Rocky Mountains. *Bull. Can. Pet. Geol.* **14**, 337 –
789 381.

790

791 Bass, B.M. 1995. Comment: transformational leadership. Looking at other
792 possible antecedents and consequences. *Journal of Management Enquiry*, **4**, 293-
793 297.

794

795 Biot, M.A. 1961. Theory of folding of stratified viscoelastic media and its
796 implications in tectonics and orogenesis. *Geological Society of America Bulletin*,
797 **72**, 1595-1620.

798

799 Bond, C.E., Gibbs, A.D., Shipton, Z.K. and Jones, S., 2007. What do you think this
800 is? 'Conceptual uncertainty' in geoscience interpretation. *GSA today*, **17**, 4.

801

802 Boyer, S.E. 1986. Styles of folding within thrust sheets: examples from the
803 Appalachian and Rocky Mountains of the USA and Canada. *Journal of Structural*
804 *Geology*, **8**, 325-339.

805

806 Boyer, S.E. and Elliott, D. 1982. Thrust systems. *Bulletin of the American*
807 *Association of Petroleum Geologists*, **66**, 1196-1230.

808

809 Brandes, C., Tanner, D.C., 2014. Fault-related folding: A review of kinematic
810 models and their application. *Earth Science Reviews*, **138**, 352-370.

811

812 Butler, R.W.H. 1986. Thrust tectonics, deep structure and crustal subduction in
813 the Alps and Himalayas. *Journal of the Geological Society, London*, **143**, 857-873.

814

815 Butler, R.W.H. 1987. Thrust system evolution within previously rifted areas: an
816 example from the Vercors, French subalpine chains. *Memorie della Società*
817 *Geologica Italiana*, **38**, 5-18.

818

819 Butler, R.W.H., 1992. Evolution of Alpine fold-thrust complexes: a linked kinematic
820 approach. In: Mitra, S. and Fisher, G. (eds.) *Structural geology of fold and thrust belts*,
821 Johns Hopkins University Press, Baltimore, 29-44.

822

823 Butler, R.W.H. 2013. Area balancing as a test of models for the deep structure of
824 mountain belts, with specific reference to the Alps. *Journal of Structural Geology*,
825 **52**, 2-16.
826

827 Butler, R.W.H. and Bowler, S. 1995. Local displacement rate cycles in the life of a
828 fold-thrust belt. *Terra Nova*, **7**, 408-416.
829

830 Butler, R.W.H., Bond, C.E., Cooper, M.A. and Watkins, H.M. 2018. Interpreting
831 structural geometry in fold-thrust belts: why style matters. *Journal of Structural*
832 *Geology*, **114**, 251-273.
833

834 Buxtorf, A. 1916. Prognosen und Befunde beim Hauensteinbasis- und
835 Grenchenbergtunnel und die Bedeutung der letzteren für die Geologie des
836 Jura gebirges. *Verh. Naturforsch. Ges. Basel*, **27**, 185-254.
837

838 Cartwright, J.A., Trudgill, B.D. and Mansfield, C.S. 1995. Fault growth by
839 segment linkage: an explanation for scatter in maximum displacement and trace
840 length data from the Canyonlands Grabens of SE Utah. *Journal of Structural*
841 *Geology*, **17**, 1319-1326.
842

843 Casey, M. and Butler, R. W. H. 2004. Modelling approaches to understanding fold
844 development: implications for hydrocarbon reservoirs. *Marine and Petroleum*
845 *Geology*, **21**, 933-946.
846

847 Cobbold, P.R. 1975. Fold propagation in single embedded layers. *Tectonophysics*,
848 **27**, 333-351.
849

850 Cooley, M.A, Price, R.A, Dixon, J.M., and Kyser T.K. 2011. Along-strike variations
851 and internal details of chevron-style, flexural-slip thrust-propagation folds
852 within the southern Livingstone Range anticlinorium, a paleohydrocarbon
853 reservoir in southern Alberta Foothills, Canada. *Bulletin of the American*
854 *Association of Petroleum Geologists*, **95**, 1821-1849.
855

856 Cosgrove, J.W. and Ameen, M.S. 1999. A comparison of the geometry, spatial
857 organization and fracture patterns associated with forced folds and buckle folds.
858 In: Cosgrove, J.W. and Ameen, M.S. (eds) *Forced folds and fractures*. Special
859 Publications of the Geological Society, London **169**, 7-21.
860

861 Coward, M.P. and Kim, J.H. 1981. Strain within thrust sheets. In: McClay, K.R. and
862 Price, N.J. (eds) *Thrust and Nappe tectonics*. Special Publications of the Geological
863 Society, **9**, 275-292.
864

865 Coward, M.P. and Siddans, A.W.B. 1979. The tectonic evolution of the Welsh
866 Caledonides. In: Harris, A.L., Holland, C.H. and Leake, B.E. (eds) *The Caledonides of*
867 *the British Isles – Reviewed*. Special Publications of the Geological Society, **8**, 187-
868 198.
869

870 Dahlstrom, C. D. A. 1969. Balanced cross-sections. *Canadian Journal of Earth*
871 *Sciences*, **6**, 743-757.
872

873 Dahlstrom, C. D. A. 1970. Structural geology in the eastern margin of the
874 Canadian Rocky Mountains. *Bulletin of Can. Petrol. Geol.* **18**, 332 – 406.
875

876 Darnault, R., Callot, J-P., Ballard, J-F., Fraise, G., Mengus, J-M. and Ringenbach, J-C.
877 2016. Control of syntectonic erosion and sedimentation on kinematic
878 evolution of a multidecollement fold and thrust zone: Analogue
879 modeling of folding in the southern subandean of Bolivia. *Journal of Structural*
880 *Geology*, **89**, 30-43.
881

882 Deville, E. and Sassi, W. 2005. Contrasting thermal evolution of thrust systems:
883 An analytical and modeling approach in the front of the western Alps. *American*
884 *Association of Petroleum Geologists Bulletin*, **90**, 887-907.
885

886 Dixon J.M. and Liu S. 1992. Centrifuge modelling of the propagation of thrust
887 faults. In: McClay K.R. (ed.) *Thrust Tectonics*. Springer, Dordrecht, 53-69.
888

889 Driehaus, L., Nalpas, T. and Ballard, J.F. 2014. Interaction between deformation
890 and sedimentation in a multidecollement thrust zone: analogue modelling and
891 application to the Sub-Andean thrust belt of Bolivia. *Journal of Structural Geology*,
892 **65**, 59-68.

893

894 Dubey, A.K. and Cobbold, P.R. 1977. Noncylindrical flexural slip folds in nature
895 and experiment. *Tectonophysics*, **38**, 223-239.

896

897 Elliott, D. and Johnson, M.R.W. 1980. Structural evolution in the northern part of
898 the Moine Thrust Zone, NW Scotland. *Transactions of the Royal Society,*
899 *Edinburgh: Earth Sciences*, **71**, 69-96.

900

901 Erslev, E. 1991. Trishear fault-propagation folding. *Geology*, **19**, 617-620.

902

903 Fernandez, N. and Kaus, B.J.P. 2014. Fold interaction and wavelength selection in
904 3D models of multilayer detachment folding. *Tectonophysics*, **632**, 199-217.

905

906 Fischer, M. W. and Coward, M. P. 1982. Strains and folds within thrust sheets: the
907 Heilam sheet, NW Scotland. *Tectonophysics*, **88**, 291-312.

908

909 Frizon de Lamotte, D., and Buil, D. 2002. La question des relations entre failles et
910 plis dans les zones externes des chaînes de montagnes. *Ebauche d'une histoire des*
911 *idées au cours du XX^e siècle. Comité français d'Histoire de la Géologie*
912 *3ème série*, **16**, 47-62.

913

914 Fossen, H. 2016. *Structural geology (2nd edition)*. Cambridge University Press,
915 509 pp.

916

917 Fox., F.G. 1959. Structure and accumulation of hydrocarbons in southern
918 foothills, Alberta, Canada. *Bulletin of the American Association of Petroleum*
919 *Geologists*, **43**, 992- 1025.

920

921 Geiser, P.A. 1988. The role of kinematics in the construction and analysis of

922 geological cross-sections in deformed terranes. *Geological Society of America*
923 *Special Paper*, **222**, 47-76.

924

925 Ghanadian, M., Faghih, A., Fard, I.A., Kusky, T. and Maleki, M. 2017. On the role of
926 incompetent strata in the structural evolution of the Zagros Fold-Thrust Belt,
927 Dezful Embayment, Iran. *Marine and Petroleum Geology*, **81**, 320-333.

928

929 Graham, R.H., Jackson, M., Pilcher, R. and Kilsdonk, B. 2012. Allochthonous salt in
930 the sub-Alpine fold-thrust belt of Haure Provence, France. In; Alsop, G.I., Archer,
931 S.G., Hartley, A.J., Grant, N.T. and Hodgekinson, R. (eds.) *Salt tectonics, sediments*
932 *and prospectivity*. Special Publications of the Geological Society, London, **363**,
933 595-615.

934

935 Groshong, R.H. 2015. Quality control and risk assessment of seismic profiles
936 using area-depth-strain analysis. *Interpretation*, **3**, SAA1–SAA15.

937

938 Groshong, R. H., Bond, C.E., Gibbs, A., Ratliff, R. and Wiltschko, D.V. 2012. Preface:
939 Structural balancing at the start of the 21st century: 100 years since Chamberlin.
940 *Journal of Structural Geology*, **41**, 1–5.

941

942 Heidmann, J-C., Durand, J., Mallard, P., Ballard, J-F. and Moron, J-M. 2017.
943 Discovery of a Bolivian Foothills giant gas field: Incahausi. *Memoir of the*
944 *American Association of Petroleum Geologists*, **113**, 153-164.

945

946 Heim, A. 1878. *Untersuchungen u̇ber den Mechanismus der Gebirgsbildung*. Benno
947 Schwabe, Basel.

948

949 Hughes, A.N. and Shaw, J.H. 2015. Insights into the mechanics of fault-
950 propagation folding styles. *Bulletin of the Geological Society of America*, **127**,
951 1752-1765.

952

953 Hughes, A.N., Benesh, N.P. and Shaw, J.H., 2014. Factors that control the
954 development of fault-bend versus fault-propagation folds: Insights from

955 mechanical models based on the discrete element method (DEM). *Journal of*
956 *Structural Geology*, **68**, 121-141.

957

958 Iacopini, D. and Butler, R.W.H. 2011. Imaging deformation in submarine thrust
959 belts using seismic attributes. *Earth and Planetary Science Letters*, **302**, 414-422.

960

961 Jamison, W.R. 1987. Geometric analysis of fold development in overthrust
962 terranes. *Journal of Structural Geology*, **9**, 207-219.

963

964 Jaquet, Y. Bauville, A. and Schmalholz, S.M. 2014. Viscous overthrusting versus
965 folding: 2-D quantitative modeling and its application to the Helvetic and Jura
966 fold and thrust belts *Journal of Structural Geology*, **62**, 25-37.

967

968 Jones Jr, S.B. and Luchsinger, A.E. 1979. *Plant systematics*. McGraw-Hill.

969

970 Kampfer, G. and Leroy, Y.M. 2012. The competition between folding and faulting
971 in the upper crust based on the maximum strength theorem. *Proceedings of the*
972 *Royal Society*, **A468**, 1280-1303.

973

974 Latham, J-P. 1985. The influence of non-linear properties and resistance to
975 bending on the development of internal structure. *Journal of Structural Geology*,
976 **7**, 225-236.

977

978 Leake, B.E., Woolley, A.R., Arps, C.E., Birch, W.D., Gilbert, M.C., Grice, J.D.,
979 Hawthorne, F.C., Kato, A., Kisch, H.J., Krivovichev, V.G. and Linthout, K. 1997.
980 Report. Nomenclature of amphiboles: report of the subcommittee on amphiboles
981 of the international mineralogical association commission on new minerals and
982 mineral names. *Mineralogical magazine*, **61**, 295-321.

983

984 Leturmy, P., Mugnier, J.L., Vinour, P., Baby, P., Coletta, B. and Chabron, E. 2000.
985 Piggyback basin development above a thin-skinned thrust belt with two
986 detachments levels as a function of interactions between tectonic and superficial
987 mass transfer: the case of the Subandean Zone (Bolivia). *Tectonophysics*, **320**, 45-

988 67.
989
990 Mancktelow, N.S. and Abbassi, M.R. 1992. Single layer buckle folding in non-
991 linear materials—II. Comparison between theory and experiment. *Journal of*
992 *Structural Geology*, **14**, 105-120.
993
994 Martin, S. 1997. Two models of educational assessment: a response from initial
995 teacher education: if the cap fits.... *Assessment and Evaluation in Higher*
996 *Education*, **22**, 337-343.
997
998 McQuarrie, N. and Ehlers, T.A. 2017. Techniques for understanding fold-and-
999 thrust belt kinematics and thermal evolution. In: Law, R.D., Thigpen, J.R.,
1000 Merschat, A., Stowell, H. and Bailey C. (eds) *Linkages and Feedbacks in Orogenic*
1001 *Process: A volume in Honor of Robert D Hatcher Jr.* Memoir of the Geological
1002 Society of America, **213**, 25-54.
1003
1004 Mitra, G. 1994. Strain variations in thrust sheets across the Sevier fold-and-
1005 thrust belt (Idaho, Utah-Wyoming): implications for section restoration and
1006 wedge taper evolution. *Journal of Structural Geology*, **16**, 585-602.
1007
1008 Mitra, S. 1990, Fault-Propagation Folds: Geometry, kinematic evolution, and
1009 hydrocarbon Traps. *American Association of Petroleum Geologists Bulletin*, **74**,
1010 921-945.
1011
1012 Mitra, S. 2003. A unified kinematic model for the evolution of detachment folds.
1013 *Journal of Structural Geology*, **25**, 1659-1673.
1014
1015 Morimoto, N., 1988. Nomenclature of pyroxenes. *Mineralogy and Petrology*, **39**,
1016 55-76.
1017
1018 Morley, C.K. 1986. Vertical strain variations in the Ose-Røa thrust sheet, North-
1019 western Oslo Fjord, Norway. *Journal of Structural Geology*, **8**, 621-632.
1020

1021 Morley, C.K., 1994. Fold-generated imbricates: examples from the Caledonides of
1022 Southern Norway. *Journal of Structural Geology*, **16**, 619-631.

1023

1024 Moutereau, F., Lacombe, O., Tensi, J., Bellahsen, N., Kargar, S. and Amrouch, K.
1025 2007. Mechanical constraints on the development of the Zagros folded belt
1026 (Fars). In: Lacombe, O., Lavé, Roure, F. and Verges, J. (eds.) Thrust belts and
1027 foreland basins: from fold kinematics to hydrocarbon systems. Springer, Berlin,
1028 247-266.

1029

1030 Mynatt, C.R., Doherty, M.E. and Tweeney, R.D. 1977. Confirmation bias in a
1031 simulated research environment: an experimental study of scientific inference.
1032 *Quarterly Journal of Experimental Psychology*, **29**, 85-95.

1033

1034 Nickerson, R.S. 1998. Confirmation bias: a ubiquitous phenomenon in many
1035 guises. *Review of General Psychology*, **2**, 175-220.

1036

1037 Nicolas, A. and Poirier, J.P. 1976. *Crystalline plasticity and solid state flow in*
1038 *metamorphic rocks*. Wiley, London, pp. 444.

1039

1040 O'Mahony, S. 2017. Medecine and the McNamara fallacy. *Journal of the Royal*
1041 *College of Physicians of Edinburgh*, **47**, 281-287.

1042

1043 Oveisi, B., Lavé, J. and van der Beek, P. 2007. Rates and processes of active folding
1044 evidenced by Pleistocene terraces at the central Zagros front (Itan). In: Lacombe,
1045 O., Lavé, J., Roure, F. and Verges, J. (eds.) Thrust belts and foreland basins: from
1046 fold kinematics to hydrocarbon systems. Springer, Berlin, 267-287.

1047

1048 Parish, M. 2015. Changes in structural style along the frontal Papuan fold belt
1049 from seismic imaging. *American Association of Petroleum Geologists data pages*,
1050 pp. 25.

1051

1052 Poblet, J. and McClay, K. 1996. Geometry and kinematics of single-layer
1053 detachment folds. *Bulletin of the American Association of Petroleum Geologists*,
1054 **80**, 1085-1109.
1055

1056 Price, N.J. and Cosgrove, J.W. 1990. *Analysis of Geological Structures*. Cambridge
1057 University Press, 502 pp.
1058

1059 Ramberg, H. 1966. Experimental models of fold mountains. Geologiska
1060 Föreningen i Stockholm Förhandlingar 87, 484-491.
1061

1062 Ramsay, J.G. 1967. *Folding and fracturing of rocks*. McGraw-Hill, New York, pp.
1063 568.
1064

1065 Ramsay, J.G. 1989. Fold and fault geometry in the western Helvetic nappes of
1066 Switzerland and France and its implication for the evolution of the arc of the
1067 western Alps. In: Coward, M.P., Dietrich, D. and Park, R.G. (eds). *Alpine tectonics*.
1068 Special Publications of the Geological Society, London, **45**, 33-45.
1069

1070 Ramsay, J.G. and Huber, M.I. 1987. *The techniques of modern structural geology*.
1071 *Volume 2: folds and fractures*. Academic Press, London, 309- 700.
1072

1073 Reber, J.E., Schmalholz, S.M. and Burg, J-P. 2010. Stress orientation and fracturing
1074 during three-dimensional buckling: Numerical simulation and application to
1075 chocolate-tablet structures in folded turbidites, SW Portugal. *Tectonophysics*,
1076 **493**, 187-195.
1077

1078 Rich, J.L. 1934. Mechanics of low-angle overthrust faulting as illustrated by
1079 Cumberland thrust block, Virginia, Kentucky and Tennessee. *American*
1080 *Association of Petroleum Geologists Bulletin*, **18**, 1584-1596.
1081

1082 Rocha, E. and Cristallini, E.O. 2015. Controls on structural styles along the
1083 deformation front of the Subandean zone of southern Bolivia. *Journal of*
1084 *Structural Geology*, **73**, 83-96.

1085

1086 Schmalholz, S.M. 2008. 3D numerical modeling of forward folding and reverse
1087 unfolding of a viscous single-layer: Implications for the formation of folds and
1088 fold patterns. *Tectonophysics*, **446**, 31–41.

1089

1090 Shaw, J., Connors, C., Suppe, J. (eds.) 2005. Seismic interpretation of contractional
1091 fault-related folds. *American Association of Petroleum Geologists Studies in Geology*
1092 **53**, pp. 156.

1093

1094 Simpson, G.D.H. 2009. Mechanical modelling of folding versus faulting in brittle–
1095 ductile wedges. *Journal of Structural Geology*, **31**, 369-381.

1096

1097 Smart, K.J., Ferrill, D.A., Morris, A.P., McGinnis, R.N. 2012. Geomechanical
1098 modeling of stress and strain evolution in contractional fault-related folding.
1099 *Tectonophysics*, **576-577**, 171-196.

1100

1101 Stearns, D.W. 1978. Faulting and forced folding in the Rocky Mountain foreland.
1102 *Geological Society of America Memoir*, **151**, 1-38

1103

1104 Suppe, J. 1983. Geometry and kinematics of fault bend folding. *American Journal*
1105 *of Science*, **283**, 648-721.

1106

1107 von Tscharnier, M., Schmalholz, S.M. and Epard, J-L. 2016. 3-D numerical models
1108 of viscous flow applied to fold nappes and the Rawil depression in the Helvetic
1109 nappe system (western Switzerland). *Journal of Structural Geology*, **86**, 32-46.

1110

1111 Williams, G. D. and Chapman, T. J. 1983. Strains developed in the hangingwalls of
1112 thrusts due to their slip/propagation rate: a dislocation model. *Journal of*
1113 *Structural Geology*, **5**, 563-571.

1114

1115 Williams, G.D., Powell, C.M. and Cooper, M.A. 1989. Geometry and kinematics of
1116 inversion tectonics. In: Cooper, M.A. and Williams, G.D. (eds). *Inversion tectonics*.
1117 Special Publications of the Geological Society, London, **44**, 3-15.

1118

1119 Willis, B. 1894. *The Mechanics of Appalachian Structure*. Department of the
1120 Interior, U.S. Geological Survey. 281 pp.

1121

1122 Woodward, A.S. 1885. IV.—On the Literature and Nomenclature of British Fossil
1123 Crocodilia. *Geological Magazine*, **2**, 496-510.

1124

1125 Woodward, N.B., Gray, D.R. and Spears, D.B. 1986. Including strain data in
1126 balanced cross-sections. *Journal of Structural Geology*, **8**, 313-324.

1127

1128 **Figure captions**

1129

1130 Figure 1. Idealised fold-thrust relationships, modified after Jamison (1987).

1131

1132 Figure 2. A compilation of buckle fold concepts and results of analogue
1133 experiments. a) single layer buckle folding, with layers of increasing competence
1134 (1-5), with the matrix competence equal to that in layer 1 (modified after
1135 Ramsay 1967). b) the concept of contact strain, adjacent to a buckled single layer
1136 (modified after Ramsay 1967). c) numerical models of evolving buckled single
1137 layer (modified after Reber et al. 2010). d) result of an analogue multilayer
1138 model subjected to layer-parallel contraction that synchronously developed
1139 folds and faults (modified from a photograph by Price and Cosgrove 1990). e)
1140 evolution of stress-strain relationships during buckling, using the deformation
1141 history outlined by Casey and Butler (2004).

1142

1143 Figure 3. Complex fold-fault relationships. a) a faulted antiform hinge zone
1144 developed in turbidite sandstones, modified from a photograph by Price and
1145 Cosgrove (1990, fig. 12.26; their “accommodation faults”). b)
1146 Fold-related faulting. a) and b) illustrate idealized patterns of hinge-failure
1147 (Price and Cosgrove 1990) while (c) illustrates this behavior in nature. The
1148 figure is redrawn from a photograph from Price and Cosgrove (1990, fig 12.26).
1149 d) Subsurface interpretation of stacked thrust faults within the Ventura Avenue
1150 Anticline in California, modified after Mitra 2003, fig. 10). e) Subsurface
1151 interpretation of the Anschutz Ranch East Field in the Utah-Wyoming thrust belt,
1152 modified after Boyer (1986, fig. 16).

1153

1154 Figure 4. plan views showing the linkage of folds by lateral hinge-line
1155 propagation. a-b are redrawn from an analogue experiment using a plasticene
1156 multilayer by Dubey and Cobbold (1977).

1157

1158 Figure 5. Development of fold trains. a-b illustrates the evolution of a single
1159 experiment with increasing contraction, reported by Dixon and Lui (1992). c)

1160 and d) show the results of finite element models of folding by von Tschärner et
1161 al. (2016).

1162

1163 Figure 6. Are detachment folds and buckle folds really different? a) and b) show
1164 Groshong's (2015) conceptualization of these styles, detachment folding and
1165 buckling respectively. c) illustrates one source of confusion, arising from
1166 cropped and centred images recording experiments on analogue materials -
1167 exemplified here, retraced from photographs in Cobbold (1975; with additional
1168 annotations). The control layer (X) is encased in a lower viscosity matrix upon
1169 which was printed a passive grid (red lines) that chart the contact strain zone.
1170 One of the grid lines is identified here and correlated between deformation
1171 states (Y). The low strain state evolves into the high strain - shown here in
1172 Cobbold's framing (left side) and re-hung relative to the passive marker Y (right
1173 side). Note that the determining subsidence of synforms depends on the
1174 adopted reference frame - or "Regional". d) and e) illustrate results of Simpson's
1175 (2009) numerical modelling of fold-trains developed above a very low-viscosity
1176 decollement zone. The "Regionals" are determined using the undeformed section
1177 to the left side of each model.

1178

1179 Figure 7. The interpretation of the Incahuasi anticline in the Bolivian foothills,
1180 after Heidmann et al. (2017). a) simplified long cross-section through the thrust
1181 belt provided for context (simplified from fig. 8 of Heidmann et al. 2017). Total's
1182 evolving interpretation of the Incahuasi anticline with the acquisition of well
1183 data is shown in the remaining parts of the diagram (b-d; modified from fig. 15 of
1184 Heidmann et al. (2017). b) illustrates the pre-drill interpretation; c) shows a
1185 modified interpretation after the first well-bore; d) shows a final interpretation
1186 that incorporates information from the first well-bore and its side-track.

1187

1188 Figure 8. A reinterpretation of the Incahuasi structure as a buckle-folded
1189 multilayer - with continuity of the axial surface to depth. Contrast with the pre-
1190 drill interpretation and its evolution (Fig. 7b-d).

1191

1192 Figure 9. Evolution of fold and thrust structures in the Central Peak anticline in
1193 the Livingstone Range, Canadian Rocky Mountains foothills – modified after
1194 Cooley et al. (2011).

1195

1196 Figure 10. Interpreted cross-section through the front of the Bornes sector of the
1197 Subalpine fold and thrust belt of the French Alps (modified after Butler et al.
1198 2018).

1199

1200 Figure 11. The nucleation of anticlines on pre-existing heterogeneities. These
1201 two examples come from the western Alps and show the Urgonian limestone
1202 (Hauterivian-Barremian) which is generally assumed to form a competent
1203 formation within an alternating series of limestones and shales (control bed in
1204 the sense of Price and Cosgrove 1990). a) interpreted cross-section from the Col
1205 de la Bataille, Vercors, France. b) annotated photograph from the Col de
1206 Sanetsch, Switzerland (visible cliff-height c 700m, to the summit of Spitzhorn).

1207

1208 Figure 12. Conceptual fold nucleation on pre-existing structures and the lateral
1209 propagation of fold hinge lines – shown here in plan view of the top of a control
1210 unit. a) shows the initial distribution of minor normal faults that will serve to
1211 nucleate the initial fold clusters (b). c) shows the lateral propagation of these
1212 hinge lines into previously unfaulted parts of the horizon. Considerations of
1213 cross-sections in these unfaulted areas would fail to identify the full causes of
1214 fold development.

1215

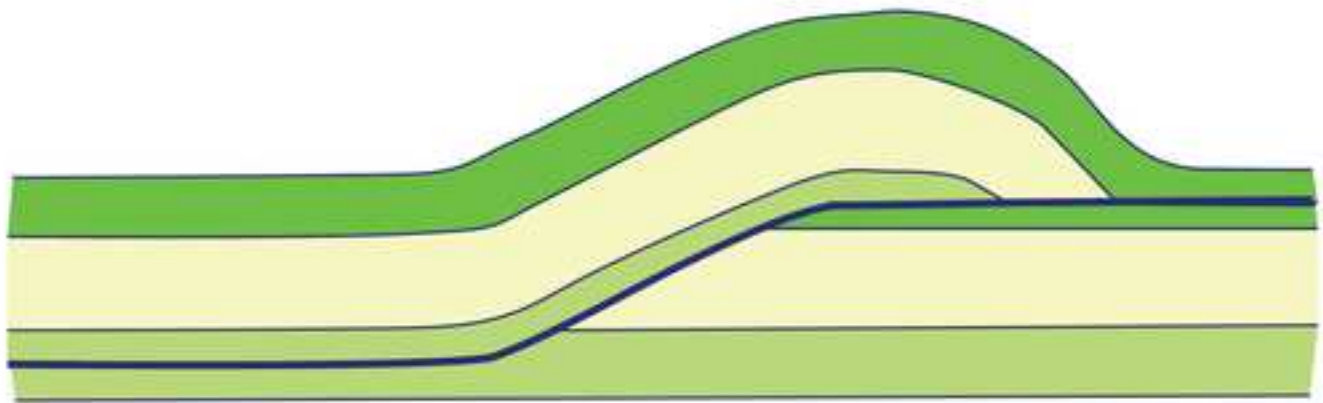
1216 Figure 13. Buxtorf's (1916) oft-reproduced cross-section through the Jura
1217 mountains of Switzerland, based on wells and railway tunnel.

1218

1219 Figure 14. A comparison of publication history of papers that cite the terms
1220 "fault-bend folding", "detachment-folding" and buckling/buckle folding. The
1221 sample was created by searching Scopus and filtering on papers classified as
1222 earth and environmental science. Papers are grouped into three-year bins.

1223

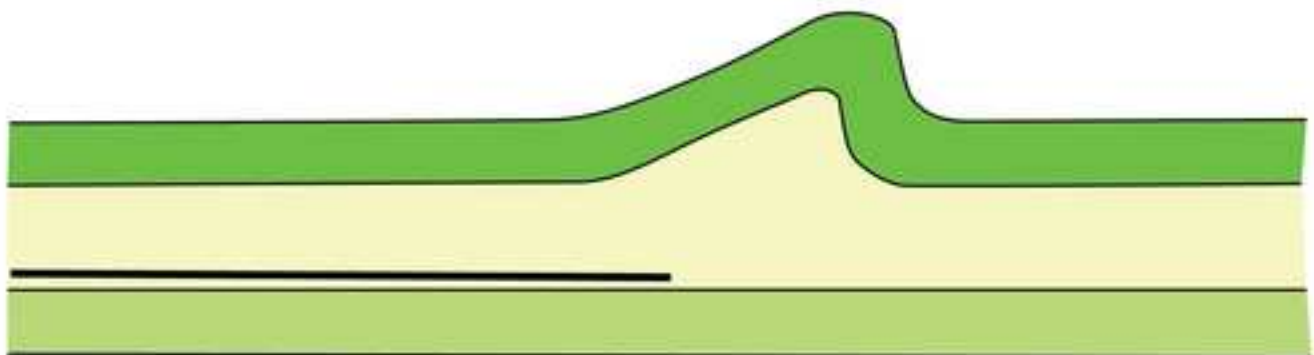
1224 Figure 15. Conceptual model for the different styles of fold-thrust structure
1225 outlined in Fig. 1, examining the pattern of distributed deformation (represented
1226 by the length of buckled bed), using the approach of Butler (1992). It illustrates
1227 the differences between “forced folding” (where deformation is solely localized
1228 on the thrust surface) and buckling. Only fault-bend folds are purely “forced” and
1229 thus only these folds are entirely fault-related. All other forms involve a
1230 component of buckling. Vertical scales refer to number of papers per 3-year bin,
1231 coded to the type of fold.



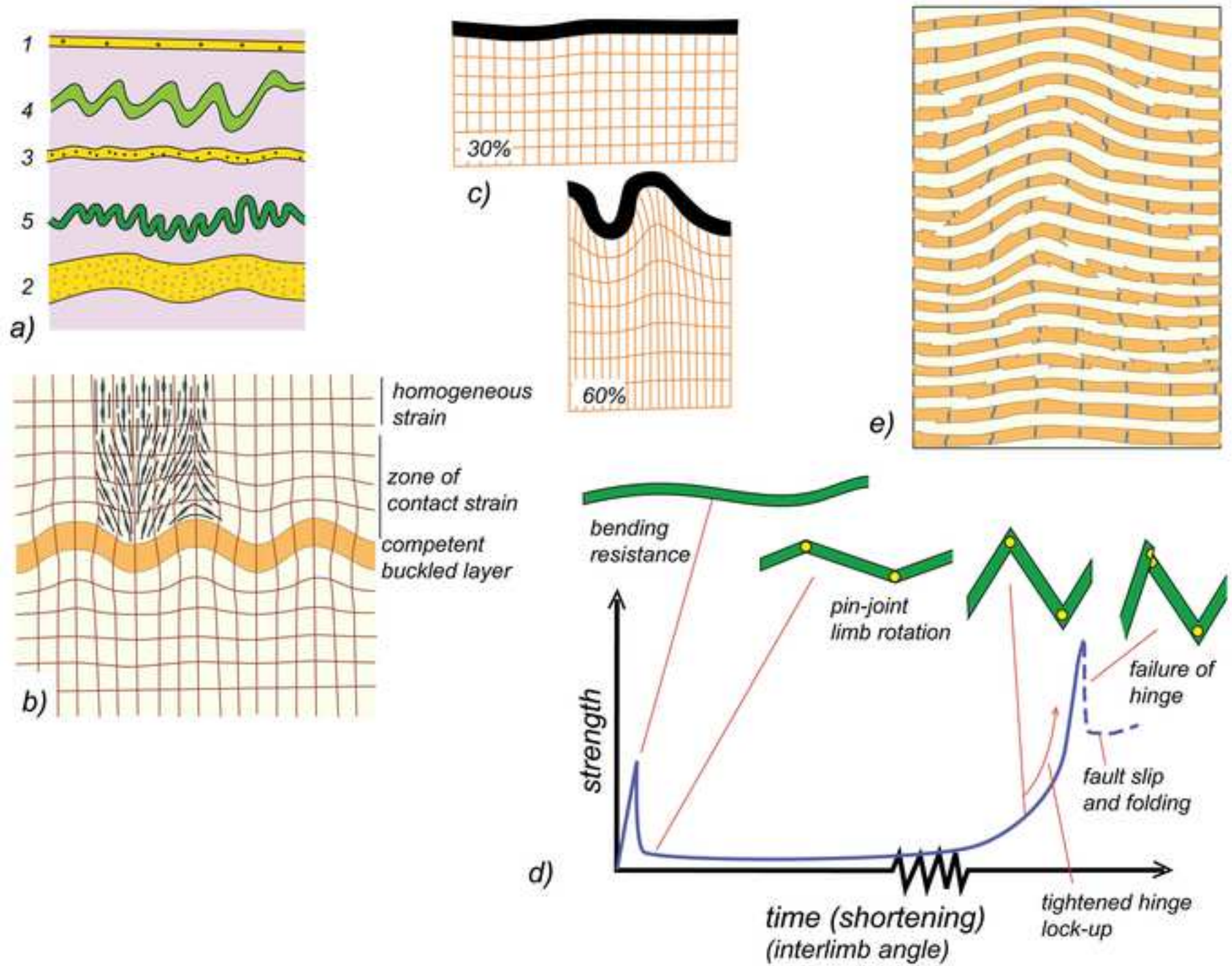
a) *fault-bend fold*

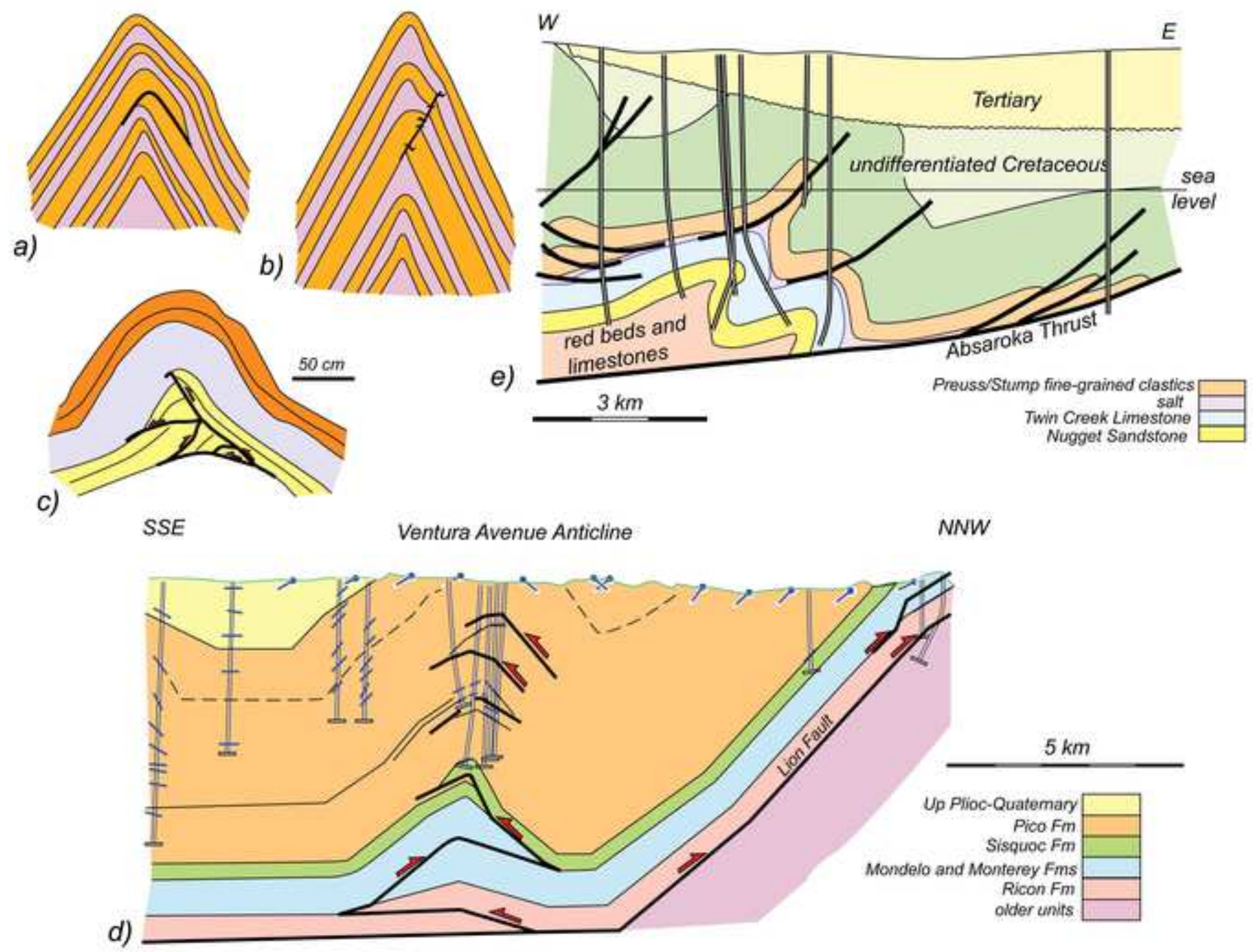


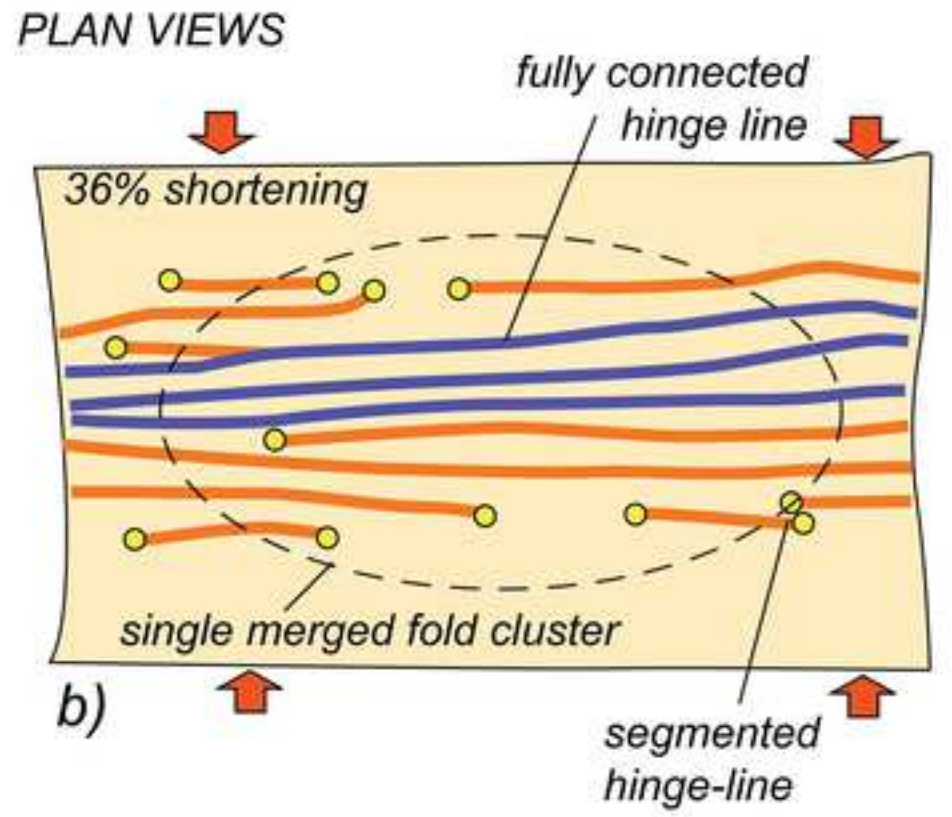
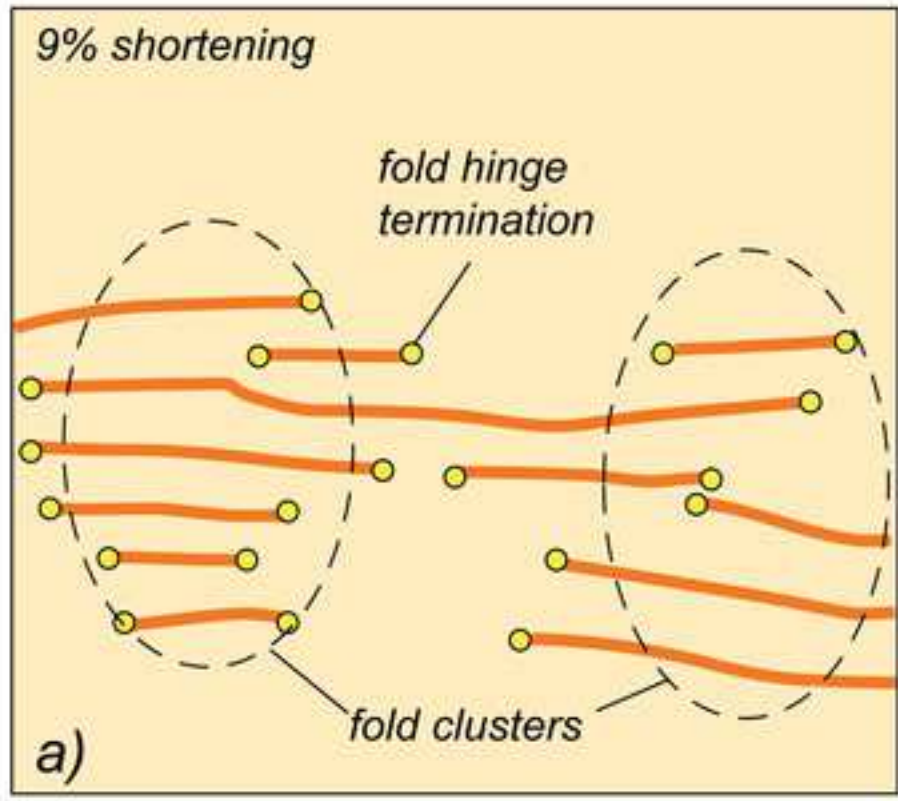
b) *fault-propagation fold*

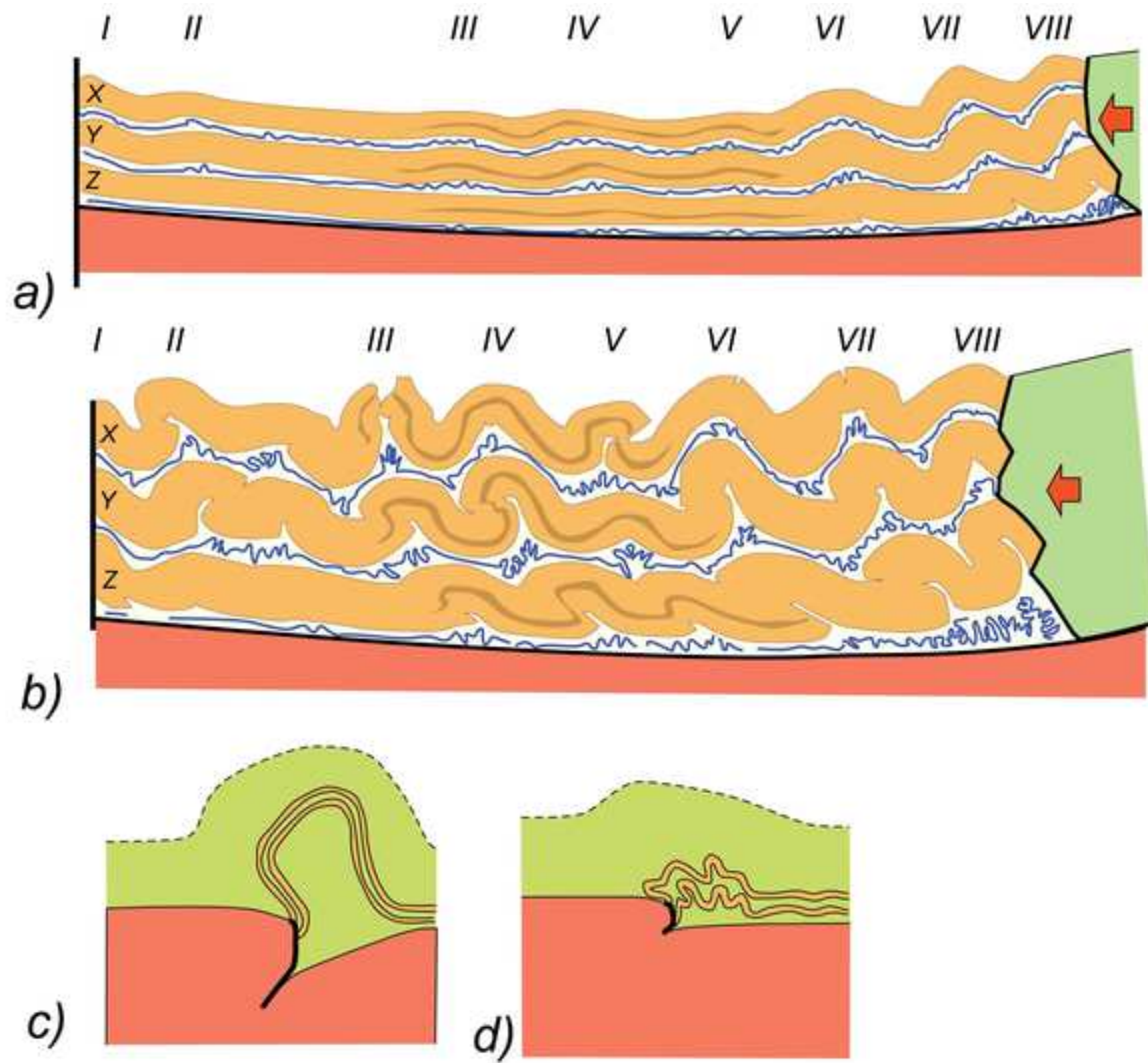


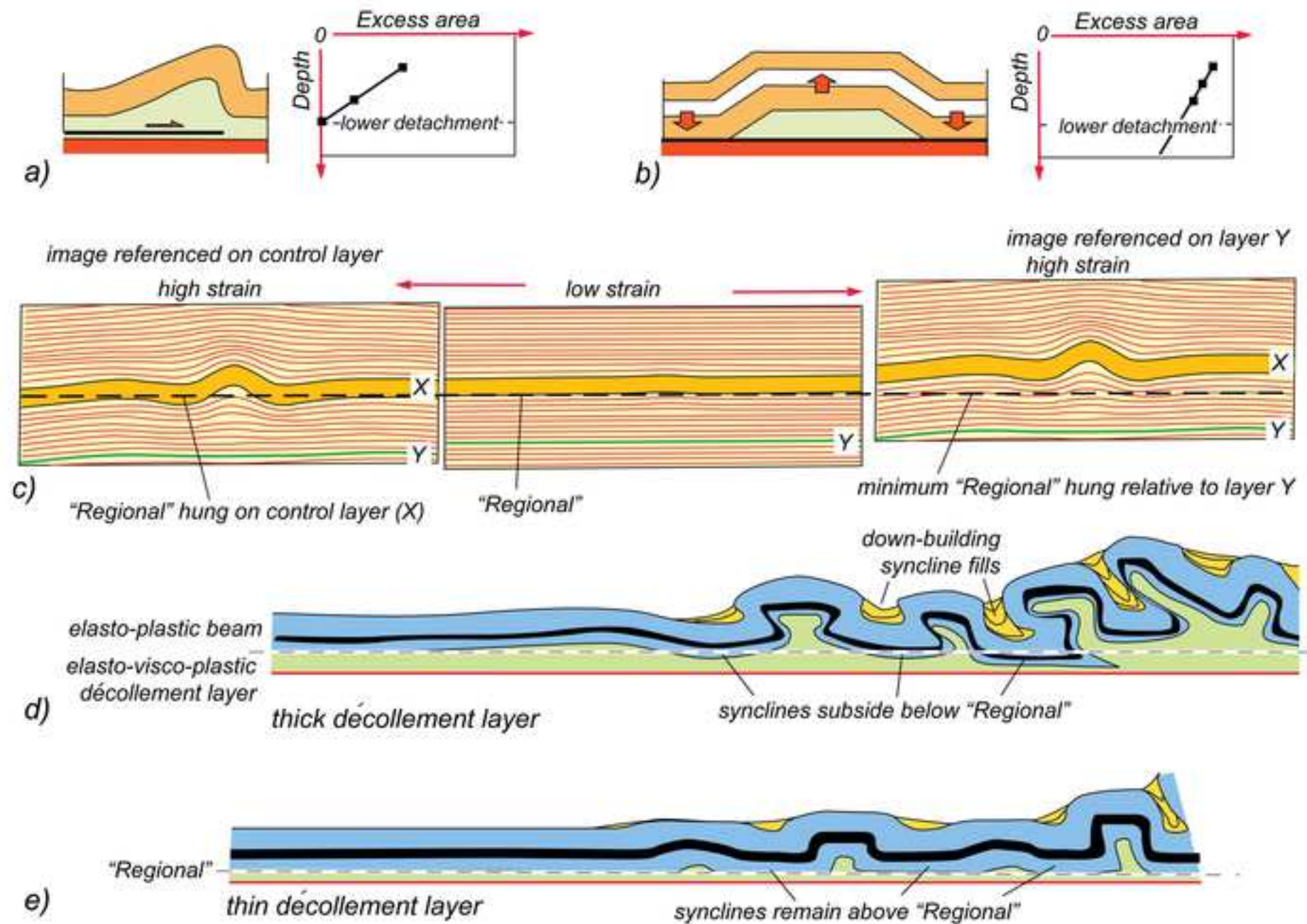
c) *detachment fold*

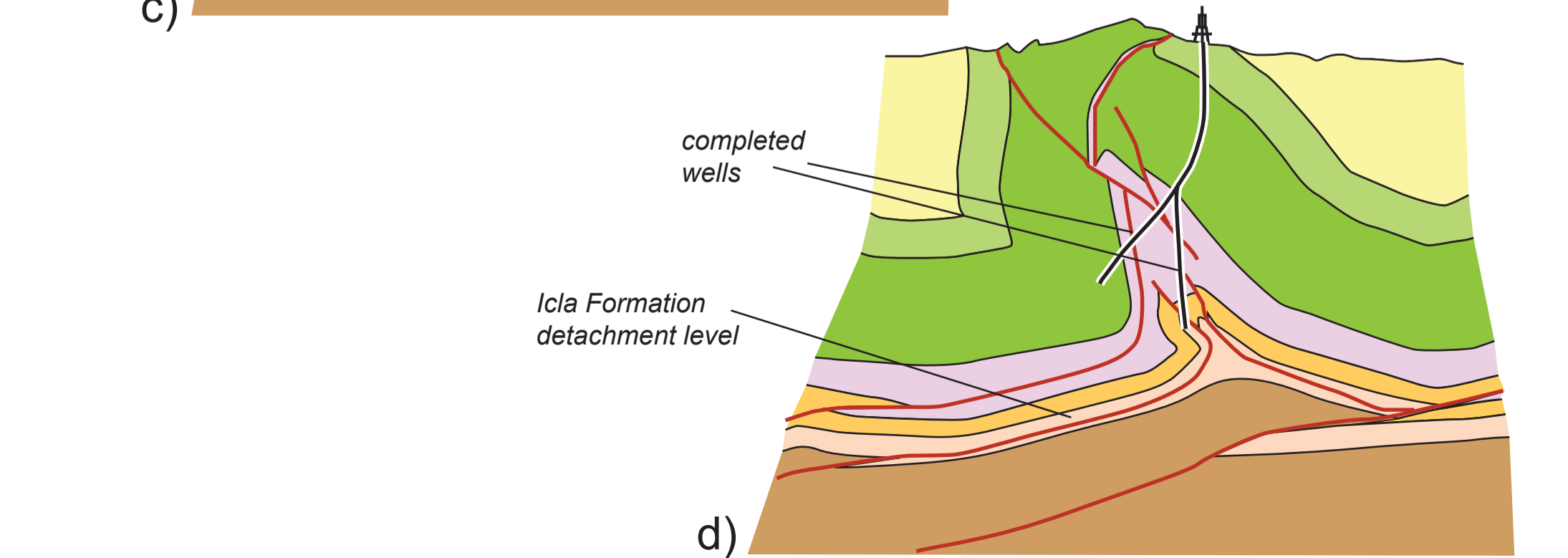
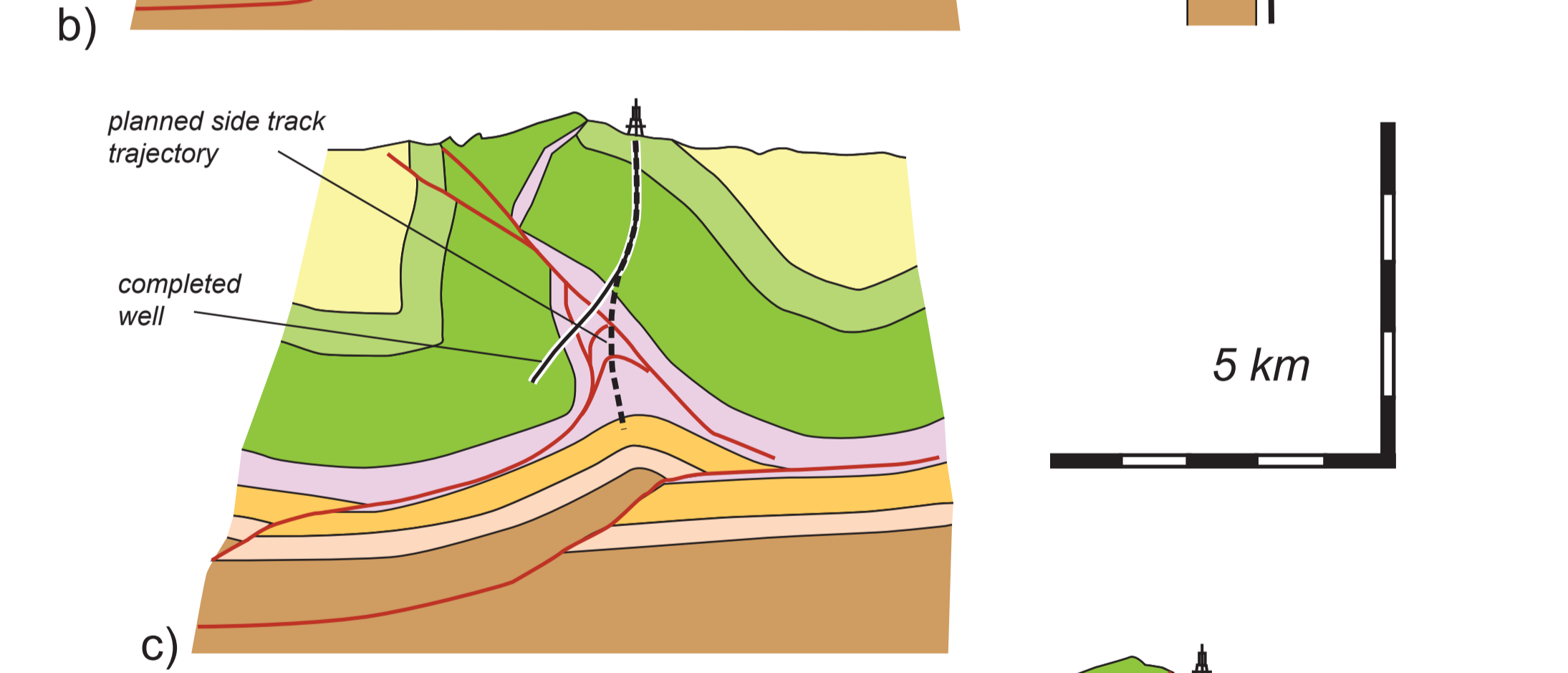
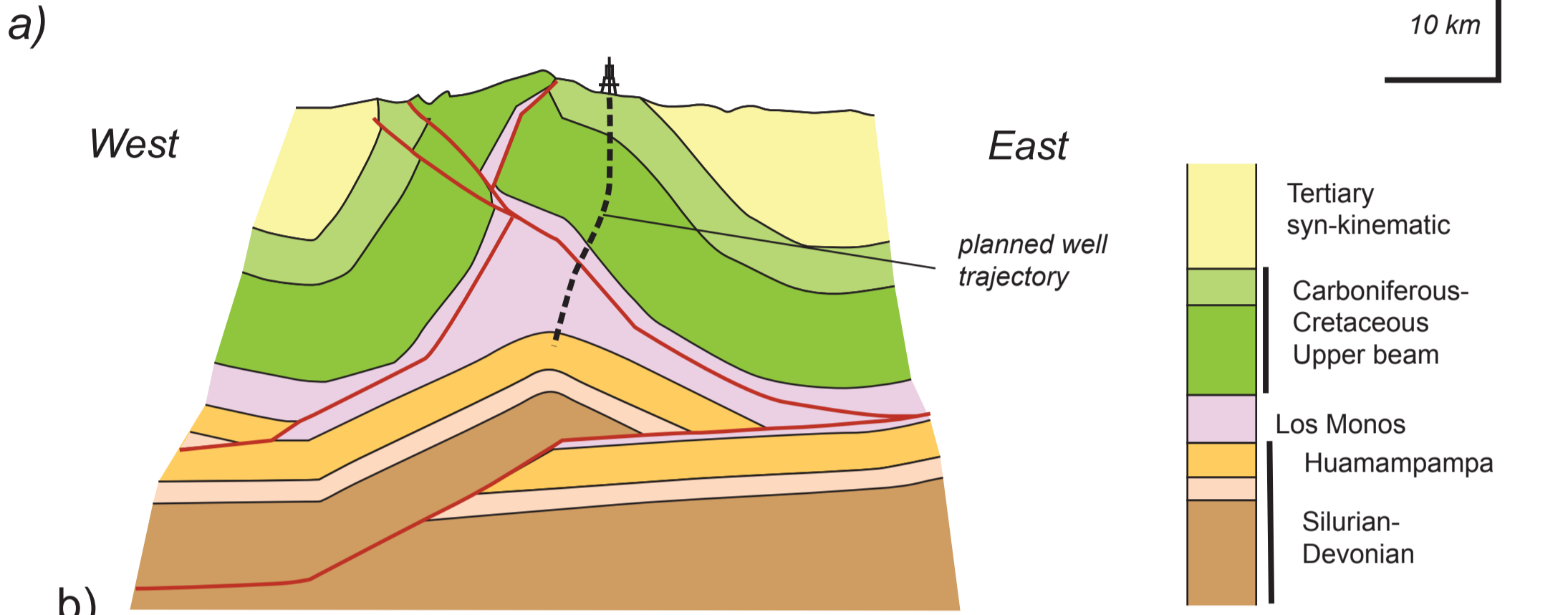
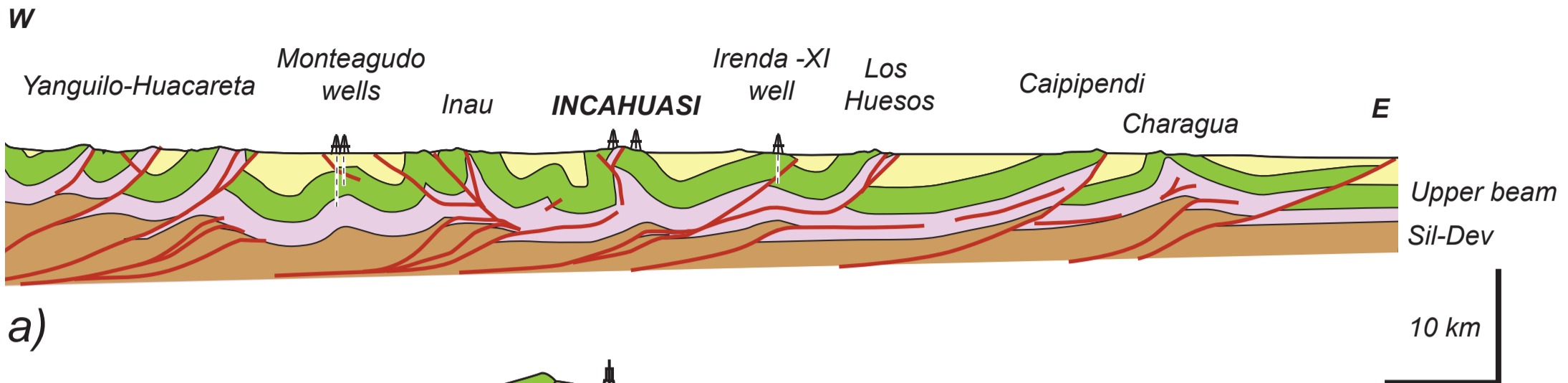


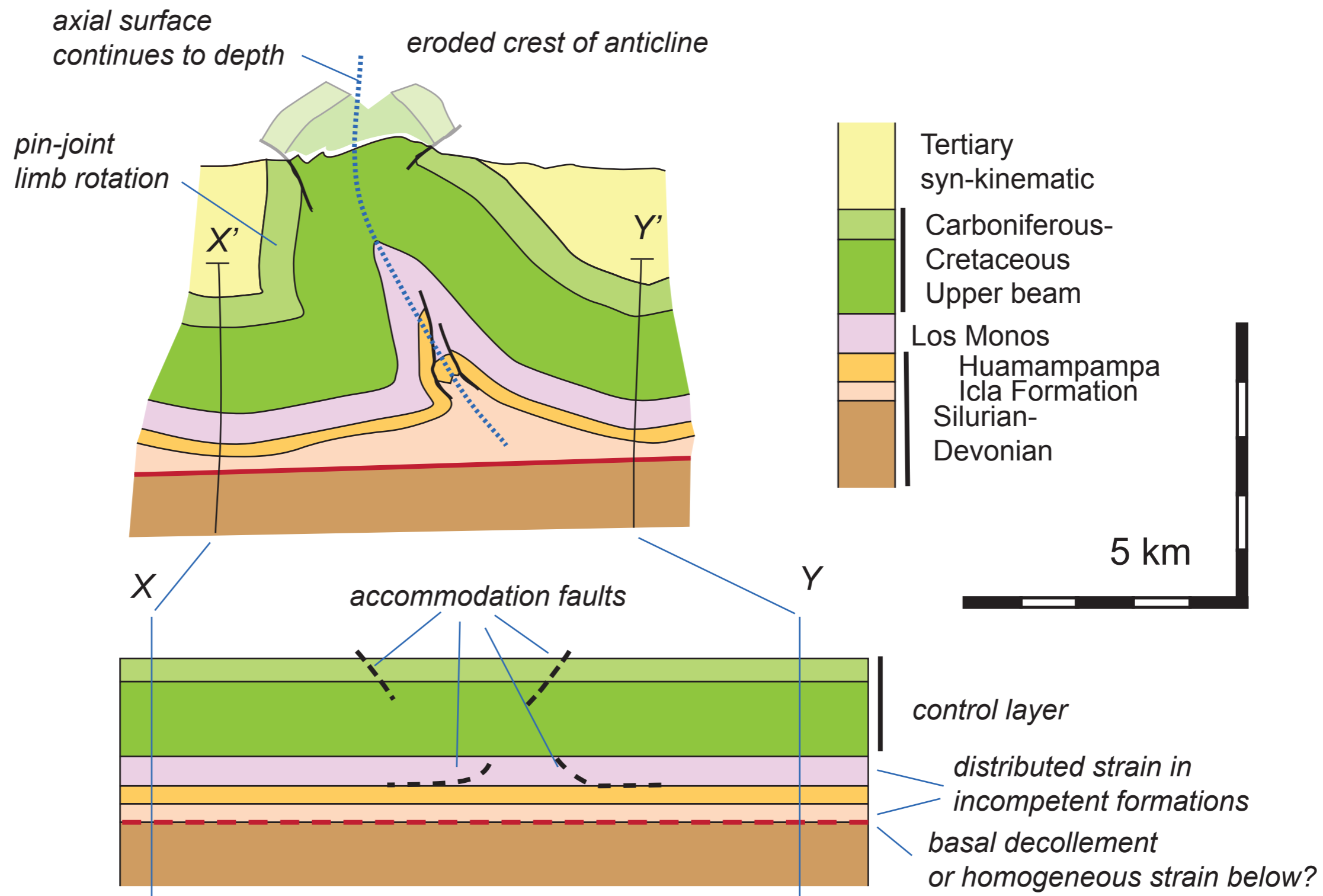


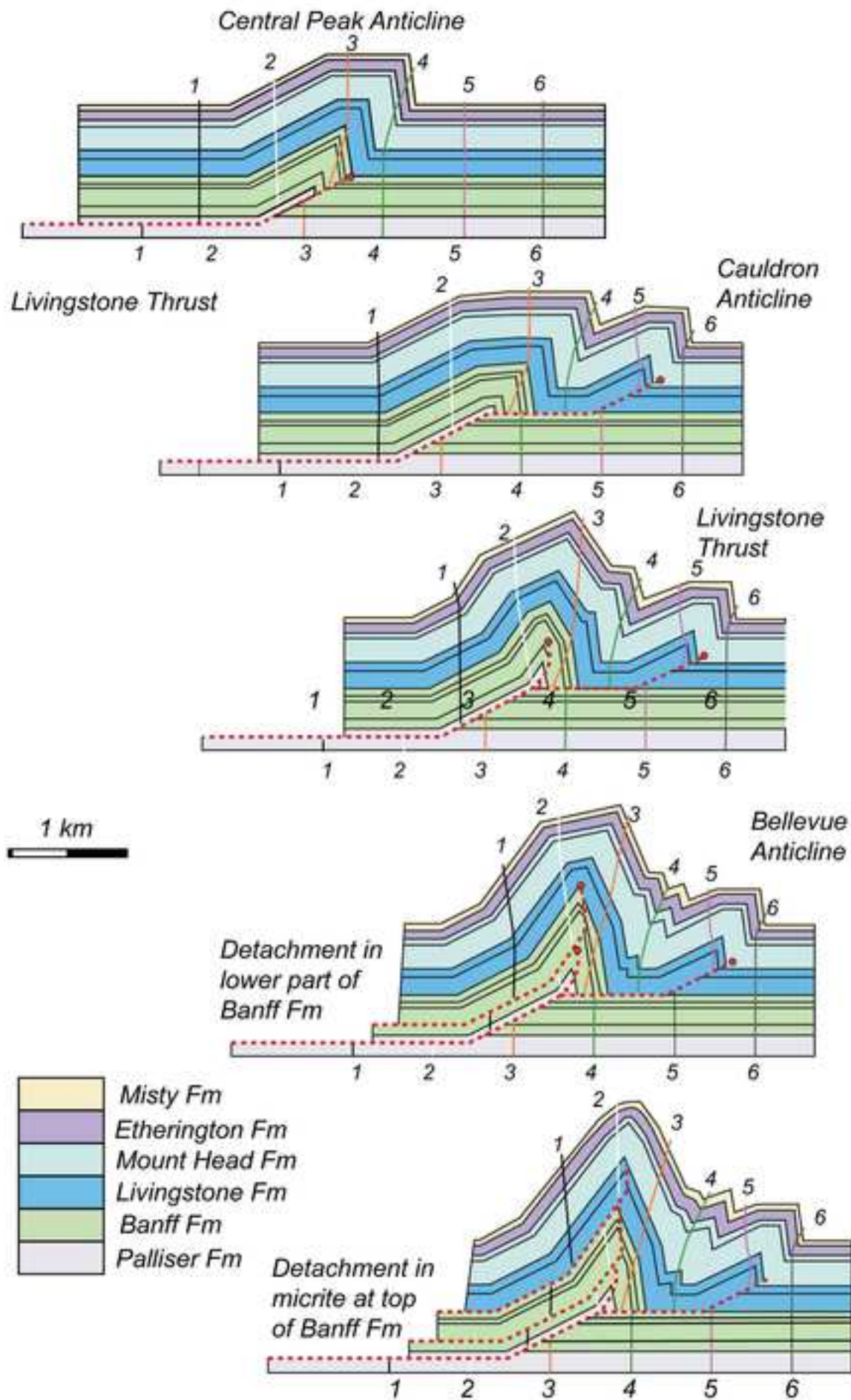


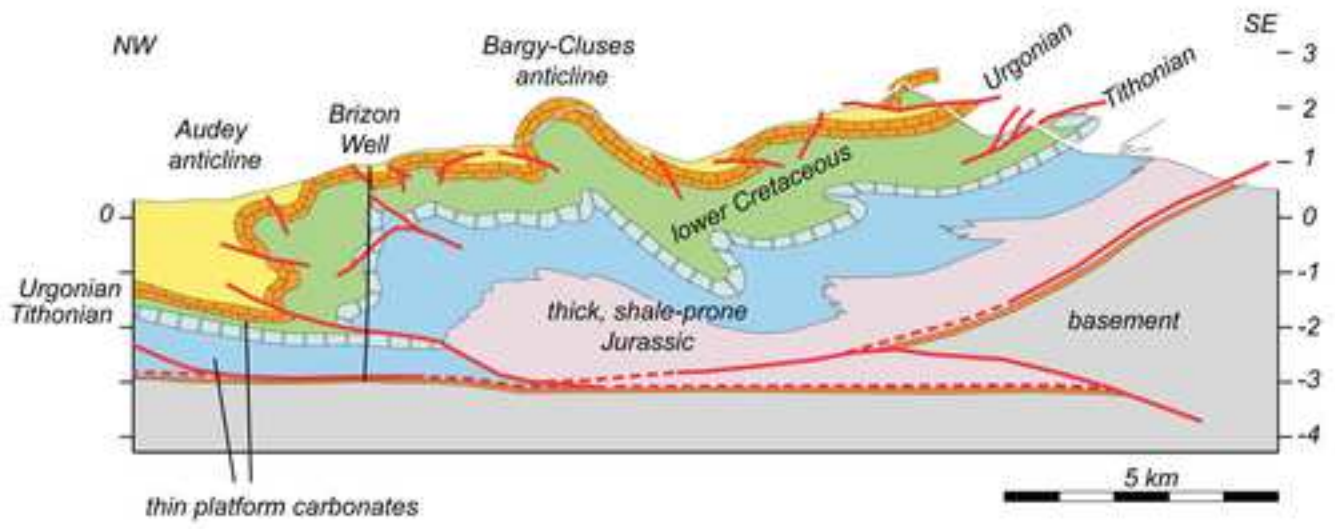


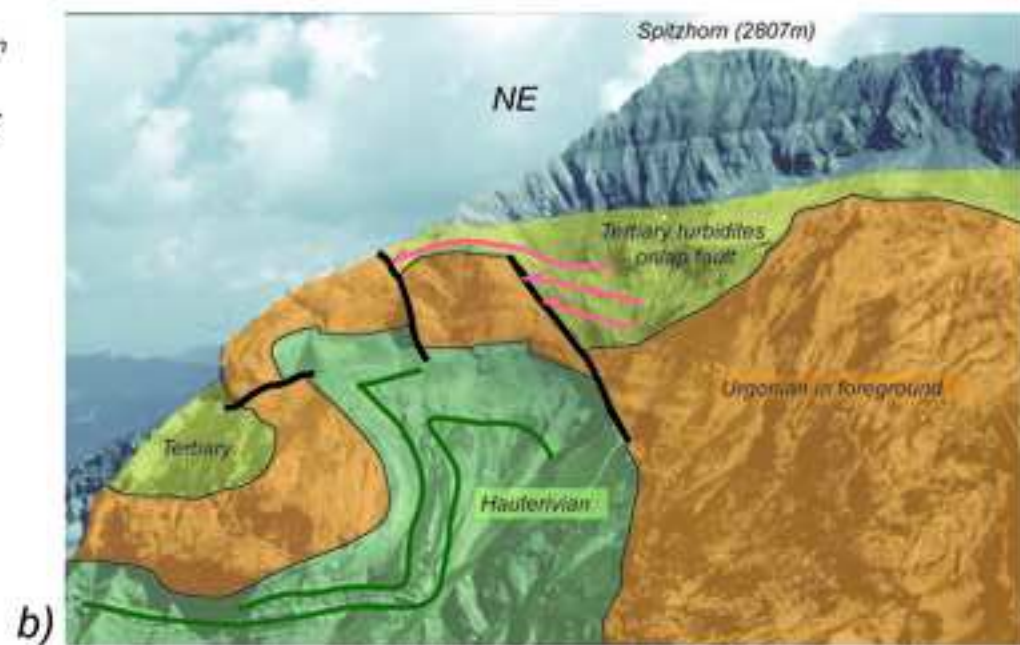
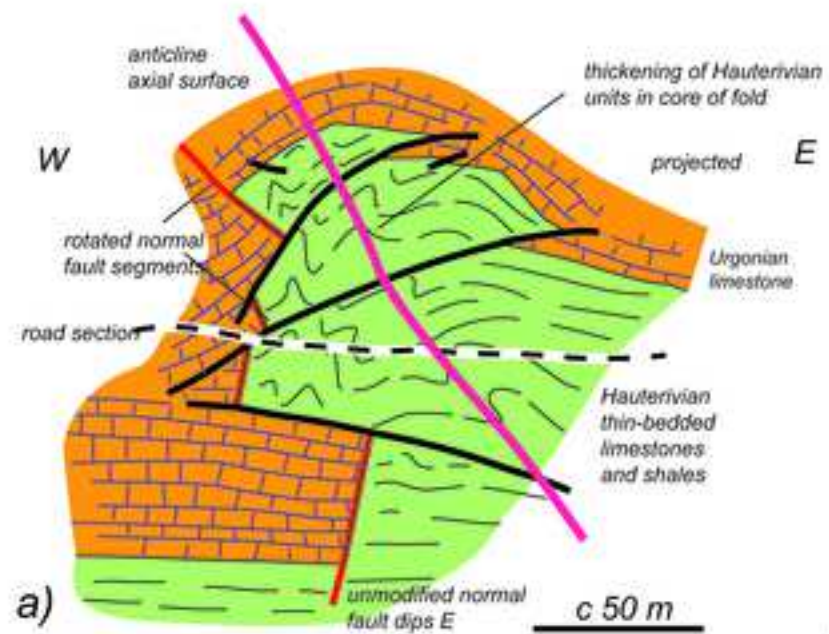


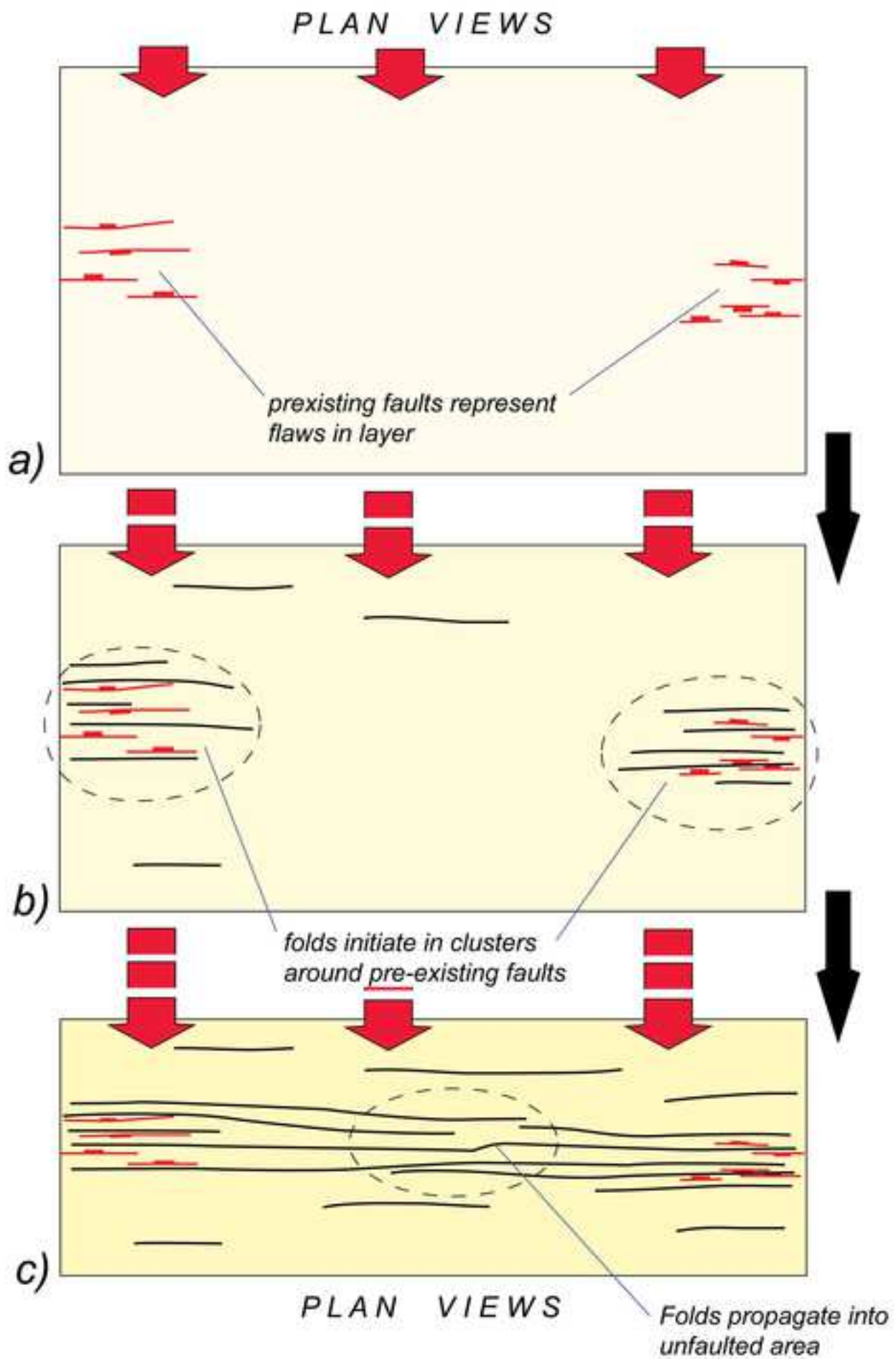


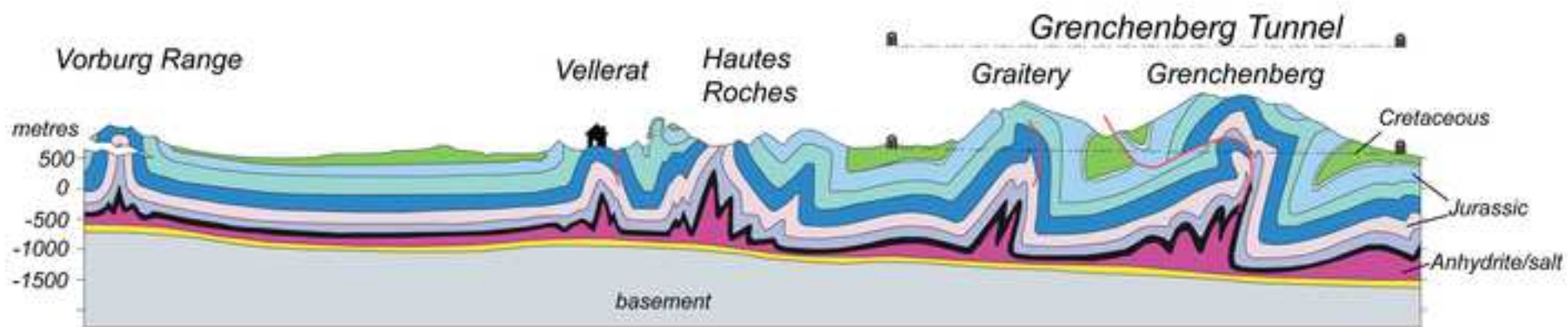


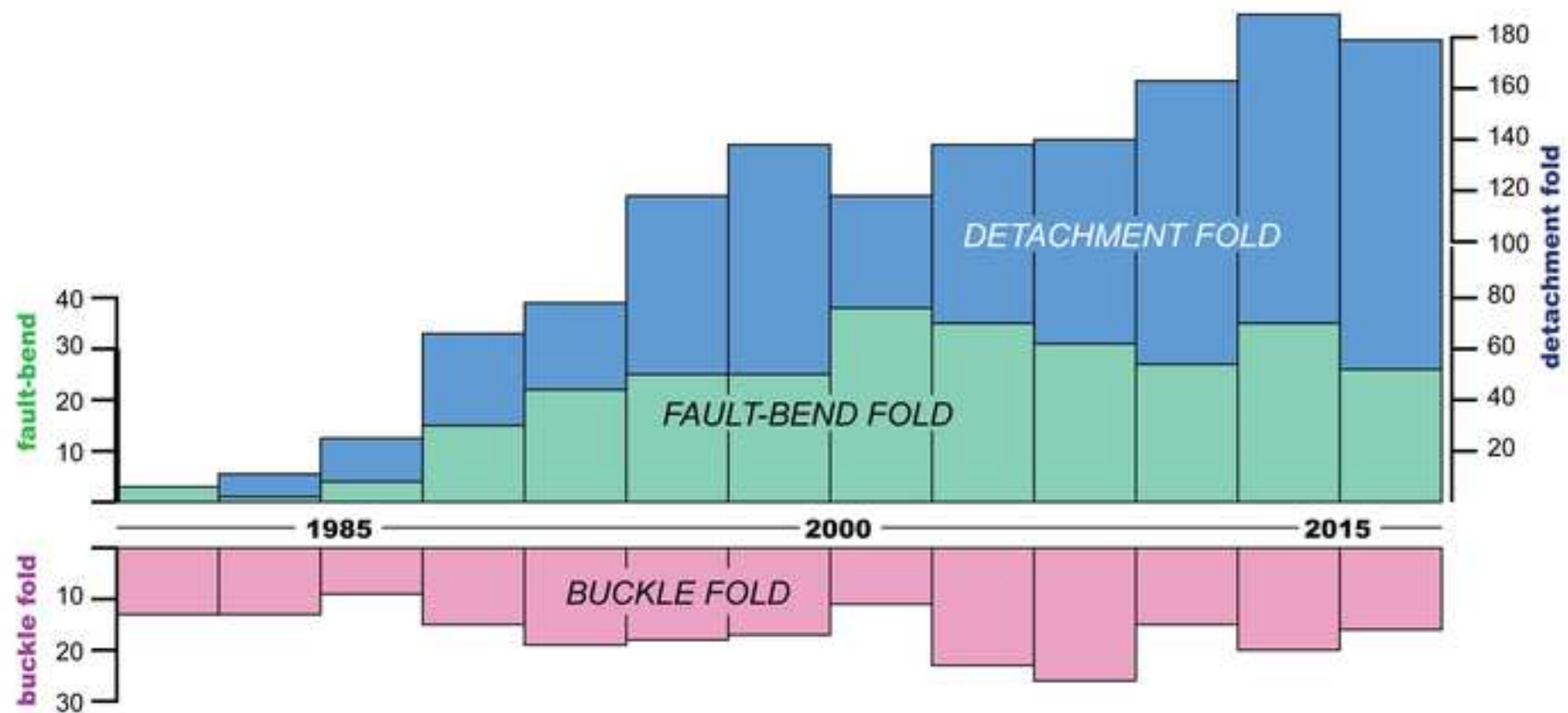




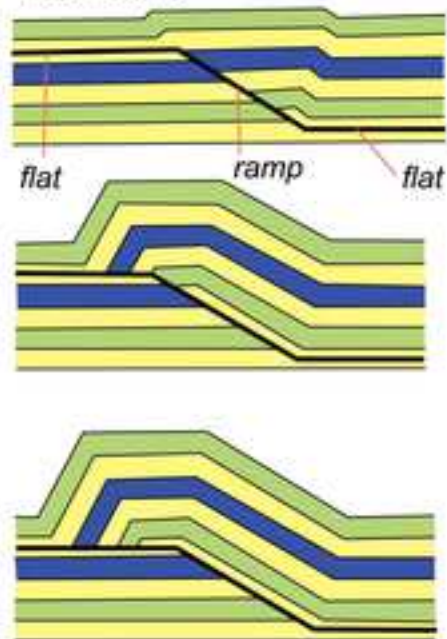




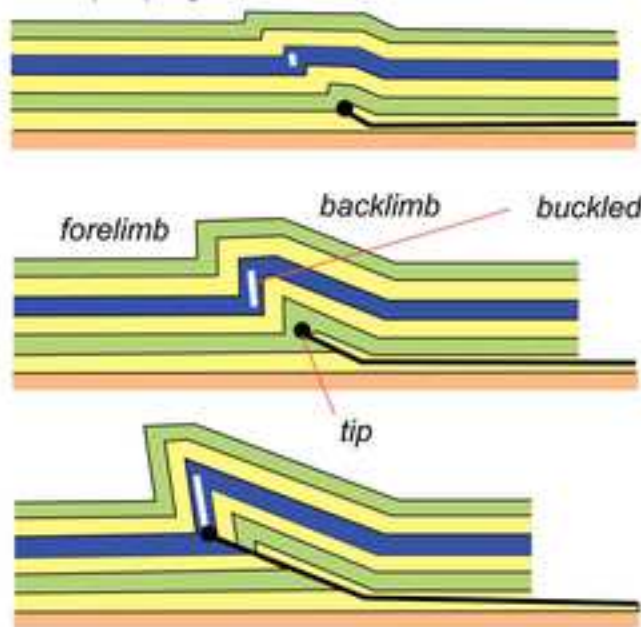




100% forced fold:
fault-bend



evolving mode:
fault-propagation fold



100% buckle fold

